MINISTÉRIO DA CIÊNCIA E TECNOLOGIA
INSTITUTO NACIONAL DE PESQUISAS ESPACIAIS

**INPE-8135-RPQ/717**

# ENSEMBLE SIMULATION OF INTERANUAL CLIMATE VARIABILITY USING THE CPTEC/COLA ATMOSPHERIC MODEL

José Antonio Marengo
Iracema Fonseca de Albuquerque Cavalcanti
Prakki Satyamurty
Carlos Afonso Nobre
José Paulo Bonatti
Igor Trosnikov
Antonio Ocimar Manzi
Gilvan Sanmpaio
Hélio Camargo Júnior
Marcos Barbosa Sanches
Chrstopher Alexander Castro Cunningham
Cassiano D'Almeida
Luciano Ponci Pezzi
Nuri Oyamburo Calbete

INPE
São José dos Campos
2001

## RESUMO

A variabilidade climática interanual do MCG atmosférico do CPTEC/COLA é avaliada para diversas regiões dos trópicos e extratrópicos. A avaliação foi feita para o período 1982-91 com uma rodada de 9 membros do modelo forçado pelas anomalias de temperatura da superfície (TSM) do mar observadas de todo o globo. O Brier Skill Score é usado para avaliar a precipitação simulada pelo modelo para diversas regiões da América do Sul, África e Ásia durante o pico de suas estações chuvosas. A variabilidade climática interanual no Nordeste do Brasil, Amazônia, e sul da Argentina-Uruguai e em menor grau para a precipitação para o Sahel e leste da África foram bem simuladas pelo modelo. O modelo exibe menor skill quando reproduz a variabilidade interanual da precipitação nas regiões das monções do globo e sul da África, indicando que a simulação das variações interanuais do clima nestas regiões ainda são problemáticas, possivelmente devido ao efeito de feedback da umidade do solo e da neve, que indicaria o importante papel da variabilidade climática interna nestas regiões, além da forçante externa SST na variabilidade climática. O modelo captura bem os conhecidos sinais das anomalias de precipitação e circulação do El Niño de 1982-83, indicando sua sensibilidade a uma forte forçante externa, enquanto que em anos normais, a variabilidade climática interna pode afetar a previsibilidade do clima em algumas regiões, especialmente as áreas de monções do globo.

## ABSTRACT

The interannual climate variability of the CPTEC/COLA Atmospheric GCM is assessed for several regions of the tropics and extratropics. The evaluation is made for the period 1982-91 for an ensemble run of 9 realizations of the model forced by observed global sea surface temperature (SST) anomalies. The Brier Skill Score is used to assess the precipitation simulated by the model for several regions of South America, Africa and Asia during the peak of their rainy seasons. Interannual climate variability in Northeast Brazil, Amazonia, and southern Argentina-Uruguay and to a lesser degree for Sahel and Eastern Africa rainfall are well simulated by the model. The model exhibits lower skill in reproducing interannual rainfall variability in the monsoon regions of world and southern Africa, indicating that simulation on interannual variations of climate in those regions still remains problematic, possibly due to the effect of land-surface moisture and snow feedbacks that would indicate the important role of internal climate variability in those regions, besides the SST external forcing. The model captures the well known signatures of rainfall and circulation anomalies of El Niño 1982-83, indicating its sensitivity to strong external forcing, while in normal years, the internal climate variability can affect the predictability of climate in some regions, especially the monsoon areas of the world.

## TABLE OF CONTENTS


| | | page |
|---|---|---|
| | Resumo | ii |
| | Abstract | iii |
| **1.** | **INTRODUCTION** | **1** |
| **2.** | **ON THE SIMULATION OF INTERANNUAL CLIMATE VARIABILITY** | **4** |
| **3.** | **ENSEMBLE SIMULATION AND PREDICTION OF INTERANNUAL CLIMATE VARIABILITY** | **7** |
| **4.** | **EXPERIMENT DESIGN AND METHODOLOGY** | **10** |
| **4.1.** | The CPTEC/COLA AGCM and implementation of the climate model runs | 10 |
| **4.2.** | Observational data sets and data processing | 11 |
| **4.3.** | Statistical assessment of the interannual variability of observed and modeled fields | 13 |
| **4.4.** | Global and regional analysis | 14 |
| **5.** | **RESULTS** | **16** |
| **5.1.** | Indices of interannual variability in the tropics and subtropics | 16 |
| **5.1.1.** | Indices of the Southern Oscillation and related circulation, rainfall and convection patterns. | 16 |
| **5.1.2.** | Position and intensity of the Bolivian and Tibetan upper-tropospheric anticyclones | 22 |
| **5.2.** | Precipitation | 28 |
| **5.2.1.** | Global features | 28 |
| **5.2.2.** | Interannual variability: Global, hemispheric, tropical and equatorial | 30 |
| **5.2.3.** | Zonal means | 33 |
| **5.2.4.** | Regional studies | 36 |
| **5.3.** | Skill of the model simulations | 42 |
| **5.4.** | Case studies of extreme events: the 1982/83 El Niño and 1998/89 La | |

Niña ..... 45
**5.4.1.** Large scale analysis: East-west equatorial circulation and tropical-midlatitude teleconnections..... 46
**5.4.2.** Monsoon systems in the Indian and South American sectors ..... 49
**5.4.3.** Circulation, convection and rainfall over the Amazon Basin ..... 55
**6. DISCUSSIONS ..... 59**
**7. SUMMARY AND CONCLUSIONS ..... 62**
Acknowledgements..... 66
**REFERENCES..... 67**

# CHAPTER 1

# INTRODUCTION

Global Climate Models (GCMs) are important tools for studying question related to climate variability and climate forecasting. Since the 1960's, observational and modeling studies of the ocean and atmosphere began to indicate that particular modes of the coupled ocean-atmosphere system might be predictable, including the El Niño-Southern Oscillation (Rasmusson and Carpenter, 1982; Neelin et al., 1998; Mason et al., 1999; Goddard et al., 2001). A recent review paper by Goddard et al. (2001) analyzes the theory and empirical evidence for climate predictability, and the predictions of surface boundary conditions, such as SST that drive the predictable part of the climate.

Starting on 1994, seasonal predictions are being carried out using the atmospheric model of the Brazilian Center for Weather Forecasting and Climate Studies (CPTEC), hereafter referred as the CPTEC/COLA AGCM. This model is derived from the COLA AGCM (Kinter et al., 1997; Shukla et al., 2000a, 2000b). The same model is used at CPTEC for medium-range numerical weather prediction.

The seasonal mean tropical circulation may be potentially more predictable than the middle latitude circulation as the low-frequency component of the tropical variability is primarily forced by slowly varying boundary conditions, such as sea surface temperature (SST), as supported by observational and modeling work (Lau, 1985; Latif et al., 1990; Goswami et al., 1995; Goswami, 1998). Given the correct lower boundary conditions, such as SST or ice extent, most atmospheric general circulation models (AGCM) can simulate the observed large-scale climate with better skill for some areas as compared to others, and give a useful indication of some of the observed regional and global interannual climate variations and long-term trends.

Even though the ability of a model to reproduce the observed mean interannual variability of climate is an important aspect of its performance, it is useful to know the ability of the model to reproduce specific time sequences of interannual variability at regional or global scales, and to understand if the variability is externally forced (e.g. by SST), or it results from internal dynamics with its characteristic chaotic behavior. Simulations using specified SST have an extensive history. Previous several studies on these issues include Shukla et al. (2000a, 2000b); Brankovic and Palmer (1997); Kumar and Hoerling (1998); Davies et al. (1997); Bengtsson et al. (1996); Stern and Miyakoda (1995); Brankovic et al. (1994); Kitoh (1991), as well as a host of studies derived from the Atmospheric Model Intercomparison Project (AMIP) climate simulations: Sperber et al. (1999a, 1999b); Sperber and Palmer (1996); Zwiers (1996); Gates (1992) and Gates et al. (1999).

Using ensembles of simulations from the same model, or simulations from an ensemble of models, dynamical seasonal and interannual predictions have the potential to provide probabilistic forecasts and to assess the skill of climate models. Based on the dispersion of the ensemble members it is possible to establish confidence thresholds on the seasonal forecast and to determine the skill of the model at seasonal and interannual scales. For some regions of the world, it is possible that predictability may be limited due to the chaotic variability on sub-seasonal time scales. Slowly varying components of the climate system, such as SST and land-surface interactions may predispose the chaotic modes of variability into preferred states resulting in an increased probability of, for instance, wet or dry rainy seasons depending on the sign of the forcing.

The assessment and validation implemented in this study include the assessment and validation of selected aspects of rainfall and circulation of the CPTEC/COLA AGCM. A companion paper (Cavalcanti et al., 2001) shows a description of the surface and upper-air climatology generated by this model. This validation effort

was made in order to identify climate features and possible systematic errors and biases on the modeled climate.

This paper presents an analysis of the interannual climate variability simulated by a 9-member ensemble of the CPTEC/COLA AGCM, with prescribed SST covering the period 1981-92. This period was characterized by moderate to strong El Niño Southern Oscillation (ENSO) events in 1982/93 and 1986/87, and two La Niña events in 1985/86 and 1988/89, which provide an attractive opportunity to evaluate the model's depiction of interannual variability and ENSO teleconnections.

The study focuses on the interannual variability of the regional and large-scale rainfall, convection and lower and upper-level circulation features. Issues such as modeling the interannual variations of rainfall in tropical and mid-latitude regions, or the regional circulation systems such as the South Atlantic an Pacific Convergence zones (SACZ, SPCZ), the Intertropical Convergence Zone (ITCZ), the Bolivian and Tibetan upper-troposphere anticyclones as components of the monsoon regimes in South America and Asia, respectively, and the impacts of El Niño/La Niña are discussed. We assess model skill and the predictability at regional scale, aimed at identifying the deficiencies and uncertainties of the model in the tropics and the extra-tropics in different seasons of the year. In particular, we assess the performance of the CPTEC/COLA AGCM in simulating the observed variability of climate during two extremes of the SO: the 1982/83 El Niño and the 1988/89 La Niña. We study the spread of the model simulations around the ensemble mean in order to identify the sensitivity of rainfall, convection and circulation to the SST/forcing, with a view to diagnose the potential predictability of interannual climate variability.

# CHAPTER 2

## ON THE SIMULATION OF INTERANNUAL CLIMATE VARIABILITY

Much attention has been focused on the interannual climate variability simulated by either atmospheric or coupled models. The El Niño phenomenon constitutes the strongest signal in the interannual variability of global SST and exhibits major effects on climate in many parts of the world (Ropelewski and Halpert, 1987, 1989; Trenberth et al., 1998). However, its effects in some areas are not as pronounced, and the climate in these parts of the world may instead be affected by SST variability in ocean basins other than the Pacific.

The results of several model intercomparisons as those performed for the AMIP period 1979-88 (Gates, 1992; Gates et al., 1999) have shown that there is agreement among atmospheric models in reproducing the larger variability observed over continents and oceans, and some of the models have distinctly different responses to a common SST forcing. Lau et al. (1996) indicates that on interannual time scales, the 29 AGCMs show reasonable skills in simulating the fluctuations of the Southern Oscillation and the eastward migration of the major equatorial precipitation zone during El Niño. Most models show useful rainfall prediction skill in the tropics associated with ENSO-related SST forcing. However the models do not show any useful skill for extratropical rainfall prediction from specified anomalous global SST forcing. Simulations of Northeast Brazil rainfall from 22 AMIP models as reported by Sperber and Palmer (1996) and Sperber et al. (1999a) indicate that models have the ability to simulate the observed interannual rainfall variability reasonably well.

Besides the AMIP experience, several studies have used AGCMs with time varying global SST's: (a) Lau (1985) studied the Geophysical Fluid Dynamics Laboratory (GFDL) AGCM response to observed SST in 1962-76; (b) Latif et al. (1990) and Kitoh (1991) studied the interannual variations of climate from 1970 to the late

1980's, using the SST anomalies to force the European Centre for Medium Range Weather Forecasts (ECMWF) and the Japan's Meteorological Research Institute (MRI) AGCMs, respectively; (c) Marengo et al. (1993) used the NASA-Goddard Institute for Space Studies (GISS) AGCM forced with observed SST in 1980-87. These studies, as well as several others on SST forced climate model variability (see references in Kumar and Hoerling 1997 and Goddard et al. 2001) show the ability of AGCMs in reproduced most of the main features of El Niño, such as changes in rainfall and circulation in tropical and extratropical regions, and the teleconnections between SST forcing in the equatorial Pacific and higher latitudes.

On regional scales, several studies have been devoted to simulations of the observed interannual variability of rainfall in several parts of the world, including regions where variability apparently is linked strongly to SST anomalies in tropical oceans besides the Pacific. For instance, Indian Ocean SST anomalies are critical for simulating the proper climate signal over eastern Africa (Goddard and Graham, 1999). Goswami (1998) assessed the interannual variability of the Indian monsoon in a model with focus on the internal and external forcing, and found that internal oscillations can account for a large part of the simulated monsoon variability. The tropical Atlantic Ocean has an important modulating effect on El Niño's impact over Northeast Brazil (Nobre and Shukla, 1996) and western Africa (Rowell et al., 1995).

Based on results from SSTs forced model results, McFarlane et al. (1992) and Zwiers (1996) used the Canadian Climate Centre (CCC) GCM2 study the 1979-88 evolution of seasonal temperature and circulation, and proposed a partition of the total interannual variability of a seasonal mean into (a) an external source component that reflects the signal of the prescribed boundary conditions; (b) an internal source component that contains the effects of internal boundary conditions, the atmospheric dynamics on long time scales, and weather noise.

An ensemble of 25 integrations of the CPTEC/COLA AGCM run on the simulation mode for the 1997/98 El Niño, reproduced quite well the observed rainfall anomalies in northem Northeast and southern Brazil regions (CPTEC, 1998), as well as the drought in northemmost Amazonia. These individual runs of the CPTEC/COLA AGCM have depicted quite well regional patterns such as the positive/negative rainfall anomalies over southeastern South America (Northeast Brazil) during the El Niño 1997/98 (Nobre and Cavalcanti, 1996; Cavalcanti et al., 1996, 1998, 1999). Local and central governments, and society in general are taking these forecasts more and more seriously into their planning activities.

Thus, it is suggested that interannual variations of seasonal circulation and rainfall in the tropics are largely determined by slowly varying boundary surface conditions (such as SST and land surface conditions (vegetation, ice-snow, and topography). Studies using AGCM (see reviews in Shukla et al., 2000a, 2000b) have identified model-simulated variances with interannual varying SST (signal) that were compared to the variances generated by the internal dynamics of the atmosphere alone (noise). The noise was estimated by integrating an AGCM with climatological SSTs, and repeating the runs wit slight changes in initial conditions (ensemble runs), or repeating them using several AGCMS (multimodel ensemble).

# CHAPTER 3

## ENSEMBLE SIMULATION AND PREDICTION OF INTERANNUAL CLIMATE VARIABILITY

Seasonal and interannual climate forecasts are based on the fact that slow variations on the boundary conditions, that include SST, sea ice, albedo, soil moisture and snow can have significant impacts on the evolution of the atmosphere (Brankovic et al., 1994). It is believed that in the tropics boundary conditions dominate the interannual variability, and that climate predictability is higher than in the extratropics. Even if the SST anomalies could be predicted with no error, the associated atmospheric evolution could not be determined accurately due to the chaotic nature of the atmosphere.

More recently, Shukla et al. (2000a) performed dynamical seasonal predictions using the 9-member ensemble run of the COLA AGCM for 16 winter seasons (mid-December through March 1981/82 to 1996/97). They successfully simulated seasonal-mean height anomalies over the Pacific North American region in the presence of large SST anomalies, suggesting the predominant role of tropical forcing in producing mid-latitude circulation anomalies.

Harzallah and Sadourny (1995) and Li (1999) used results of an ensemble run of the Laboratoire de Meteorologie Dinamique (LMD) AGCM forced with observed SST for different periods between 1970-89. Among other things, their model was able to reproduce the teleconnection between the tropical Pacific SST and the Northern Hemisphere circulation. Meanwhile, the study also revealed some problems with the model, mainly that the atmospheric response to the warm ENSO episode was too weak over the eastern part of the Tropical Pacific, inducing a westward shift of the PNA teleconnection pattern through the local Hadley circulation. Similar experiment was performed by Barnett (1995) using the Max Planck Institute for Meteorology ECHAM3 AGCM, and he found that the internal

model variability could be very large, and that a single model simulation of interannual climate variability or even climate forecast is totally inadequate for judging the model's abilities and skill.

In the same vein, Kawamura et al. (1997) and Yang et al. (1998) used a T42 AGCM version of the Japan Meteorological Agency, and 10-years AMIP run, respectively, to examine the extratropical interdecadal and interannual variations over the North Pacific region associated with the anomalous SST forcing in the tropics, and to assess the potential predictability of the extratropical atmospheric seasonal variations. Among other things, they found that potentially predictable regions during boreal spring and winter are confined to the traditional Pacific North America (PNA) region while during boreal summer and fall they are favored over the middle part of North America, in agreement with Shukla et al. (2000a).

Rowell (1998) assessed potential seasonal predictability with an ensemble of multidecadal runs of the Hadley Center AGCM (HADAM1), and showed that the highest predictability occurs over the tropical oceans, particularly the Pacific and Atlantic. For several of these studies the forced variability is defined as the ensemble mean, whereas the internal variability may be defined as the deviation from the ensemble mean. They show that the spread among the ensemble (indicating sensitivity to initial conditions) is as large as the interannual variability itself.

Wang and Zwiers (1999) studied the interannual variability of precipitation in an ensemble of 6-year AMIP climate simulations conducted with the CCC GCM2, for the period 1979-88. They found that precipitation frequency appears to be more sensitive to the external forcing than precipitation intensity, especially over land areas. Previously, Ward and Navarra (1997) performed an ensemble of three integrations of the ECHAM4 GCM using forced with observed SST through the 1979-88 period, and the significant reproducibility of climate anomalies in the

central and western tropical Pacific among ensemble members indicated potential seasonal forecast skill.

Due to the fact that model's internal variability can be very important, many studies use an ensemble approach to assess the atmospheric response to SST anomalies. Zwiers (1996) assessed the interannual climate variability in an ensemble of climate simulations using the CCC GCM2, and concluded that no evidence was found that the atmospheric internal dynamics on their own alone generate potential predictability variations on the interannual time scale. The idea is that climate simulation is mainly a boundary-forced problem and model internal variability can be considered as noise. Even though the causes of model internal variability are not fully known, the use of ensemble means can partly overcome the difficulties posed by the model internal variability.

# CHAPTER 4

# EXPERIMENT DESIGN AND METHODOLOGY

## 4.1 THE CPTEC/COLA AGCM AND IMPLEMENTATION OF THE CLIMATE MODEL RUNS

The dynamical core of the CPTEC/COLA AGCM is based on the COLA AGCM, described by Kinter et al. (1997). The CPTEC/COLA model includes parameterizations of solar radiative heating, terrestrial radiative heating, cloud-radiation and other processes, is discussed in Satyamurty and Bittencourt (1999) and Bonatti (1996):

| | |
|---|---|
| Name: | CPTEC/COLA AGCM |
| Type: | Numerical forecast global spectral model, with sigma coordinates and spherical horizontal coordinates |
| Origin: | NMC GCM, rhomboidal version 1.7 COLA GCM |
| Current version: | Triangular COLA GCM, user defined horizontal and vertical resolutions (T62L28) |
| Boundary | Conditions:Vertical sigma velocity null at top and surface, smoothed and truncated spectral topography, climatological zonal mean ozone concentration (each time step), NCEP weekly running mean SST, initial climatological fields: soil moisture, snow and SST. |
| Initialization: | Diabatic non linear mode |
| Spectral dynamics: | Primitive equations (vorticity and divergence), finite difference schemes at vertical and time, semi-implicit time integration and Asselin's filter |
| Physical processes: | Surface-Land SSiB, Ocean bulk aerodynamic scheme<br>Planetary Boundary layer-Vertical turbulent diffusion 2.0 of Mellor and Yamada. Gravity wave drag from NMC.<br>Radiation-Short wave every hour form Lacis and Hansen. Long wave every three hours from Harshvardhan. Cloud radiation iterations as derived by Slingo.<br>Kuo deep convection, and Tiedke shallow convection schemes.<br>Other adjustments-large scale condensation and Bi-harmonic horizontal diffusion from NMC, and local diffusion-CFL. |

We use the approach of multiple realizations as necessary to assess the robustness of the CPTEC/COLA model response to SST forcing. Using the ensemble technique, score analysis such as the Brier Skill Score (BSS) can give more confidence in the model results.

The simulation was initiated from September 11-19 1981 ECMWF operational analyses and monthly NCEP SSTs, for the 12 UTC. The ensemble is considered to be a collection of 9 independent simulations of the December 1982 to November 1991 model climate that are physically consistent with observed worldwide SST and sea-ice extent in this period.

The model's seasonal and annual climatology is defined as the mean of all ensemble members of the experiment. In all cases, simulated anomalies are defined relative to the 1982-91-model climatology, and the observed field anomalies are determined relative to the 1982-91 climatology of the NCEP/NCAR reanalysis, the CMAP precipitation data sets, and the NOAA OLR data set (see Section 4.2 for data description).

## 4.2 OBSERVATIONAL DATA SETS AND DATA PROCESSING

The pressure difference Tahiti (18 °S, 150 'W) minus Darwin (12 °S 131' W) was used as an index of the Southern Oscillation (SO) hereafter referred as SOI, during 1982-91. Prof. S. Hastenrath from the University of Wisconsin-Madison, US provided data of the SO. The high phase of the SO is defined by anomalously high/low pressure at Tahiti/Darwin. The model SOI is computed from area-averaged sea level pressure at grid points closest to the locations of Tahiti and Darwin, from the mean of the ensemble of the nine 10-year integrations.

To validate the model interannual variability, monthly circulation fields were derived from the NCEP/NCAR reanalysis (Kalnay et al., 1996). These reanalyses are a high quality data set suitable for many uses, including weather and short-term

climate research. As pointed out by Garreaud and Wallace (1998), an important caveat of the NCEP reanalysis for studies over the Southern Hemisphere involves incorrectly assimilated Australia's surface pressure bogus data (PAOBs) between 1979 and 1992. Although this error must be kept in mind in the following discussions, we are confident that the NCEP reanalysis captures most of the essential features of the large-scale circulation climatology and its interannual variability.

Global and regional rainfall was derived from the Climate Prediction Center [CPC] Merged Analysis Precipitation (CMAP) data (Xie and Arkin, 1997, 1998). The CMAP data set is constructed on a 2.5 latitude-2.5 longitude grid and covers a 20-year period from January 1979 to December 1998. This data set merged several types and sources of rainfall information, including gauge-based monthly analyses and satellite estimates, to generate a precipitation product that can be used for the study of large-scale rainfall variability. The CMAP contains the largest amount of land and satellite data. For OLR, the NOAA OLR global data set is used (Janowiak et al., 1985). To make suitable comparisons between model and the observational data sets, model output was interpolated from the T62 horizontal resolution to the 2.5 x 2.5 degrees lat-long resolution of the observations.

The validation is made for the interannual variability of climate, and for the structure of global teleconnections, with emphasis on two extremes of the ENSO cycle during 1982-1991. Extremes of the SO during the period of 1982-91 were selected as cases studies: El Niño in 1982/83 and La Niña in 1988/89. Climatic indices were constructed, and they are expressed as normalized departures. The indices were constructed from time series of rainfall, circulation, convection and temperature, and expressed as departures from the long-term monthly and/or seasonal mean for each year, and then divided by the standard deviation to normalize the time series. The word "validation" to be used here represents the degree of correspondence between model and the real world it seeks to represent.

## 4.3 STATISTICAL ASSESSMENT OF THE INTERANNUAL VARIABILITY OF OBSERVED AND MODELED RAINFALL FIELDS

The skill of the CPTEC/COLA AGCM is assessed using the Brier Score Skill or BSS (Sperber et al., 1999a; Sperber and Palmer, 1996). In previous studies, this technique has been used to analyze the ECMWF medium range ensemble forecasts system and multi-model ensemble simulations from AMIP (Sperber et al., 1999a). We assess only precipitation anomalies to derive scores in some regions of the globe: northern and southern Northeast Brazil, Amazonia, southern Brazil-Uruguay, Northwest Peru-Ecuador, Indian monsoon region, Sahel and Eastern Africa. Interannual climate variability and predictability in these regions, as well as their associations with the extremes of SO have been well documented in previous studies (Ropelewski and Halpert, 1987, 1989; Sperber and Palmer, 1996; Mason et al. 1999; Sperber et al., 1999a, 1999b).

The Brier score, here implemented as in Panofsky and Brier (1968), has been used as a measure for assessing numerical weather prediction performance. This is a binary score and is calculated as in Sperber et al. (1999a):

$$B_s = \frac{1}{n_y} \sum_{i=1}^{n_y} [(1.0 - Y_i)^2 + (0.0 - N_i)^2]$$

Where $Y_i$ is the fraction of members that correctly simulated an anomaly of the correct sign, and $N_i$ is the fraction of members that did not simulate an anomaly of the correct sign. It is required that the observed standardized departure for a given year *i* exceed +/- 0.25 to be included in the calculation of the Brier score, in which case the number of years $n_y$ over which the Brier score is calculated may be less than 10. Brier skill scores may range from 0.0 (a perfect score) to 2.0 (total disagreement with observations). The Brier score of climatological forecast is 0.5 (Sperber et al., 1999a). For a review on the BSS, the reader is referred to Storch

and Zwiers (1999, p. 396, 400-402). The BSS above defined is the Brier score for a climatological forecast, and is different from the Brier sill score defined in Shukla et al. (2000a), in which a climatological forecast of an event is the forecast in which the climatological probability is predicted.

Sperber and Palmer (1996) have shown that individual members of an ensemble are generally not robust, so scores from a single run will be a poor indication of the skill of the model, and multiple runs are needed to properly assess skill. A better score is expected for a seasonal average than for an individual monthly average. Thus, the assessment of the BSS is implemented for the rainy season of each analyzed region.

## 4.4 GLOBAL AND REGIONAL ANALYSIS

Several regions from around the globe have been chosen for assessment of the simulation and predictability. Regions such as Northwest Peru, northern Northeast Brazil, northern Amazonia, southern Brazil, East Africa, and northern Australia exhibit the impact of the extremes of the Southern Oscillation (El Niño), and in regions such as Amazonia the impact is better defined only during very strong El Niño events (Marengo, 1992; Nepstad et al., 1999). The monsoon regions of India-Southeast Asia, Australia, North and South America have been included, as well as areas of the major tropical convergence zones. Some of these areas were defined based on studies of global impacts of the extremes of ENSO by Ropelewski and Halpert (1987, 1989) and by regional studies in Brazil, developed at CPTEC during the last 10 years. Rainfall variability shows a strong association with the occurrence of ENSO, and this association indicates a teleconnection between ENSO and rainfall in this region through the Indian Ocean (Mason et al., 1999).

Fig. 4.1 shows the location of these 15 areas and the analysis is based on the 1982-1991 interannual variability of the peak of the respective rainy season. For

some regions in South America, a special comparison is made for the two case studies, representative of the extremes of the Southern Oscillation. Where appropriate, we also compare the model results with those from previous observational studies using other long-term historical climatic data sets (Legates and Willmot, 1990), or those derived from AMIP that may include the 1982-91 period analyzed here.

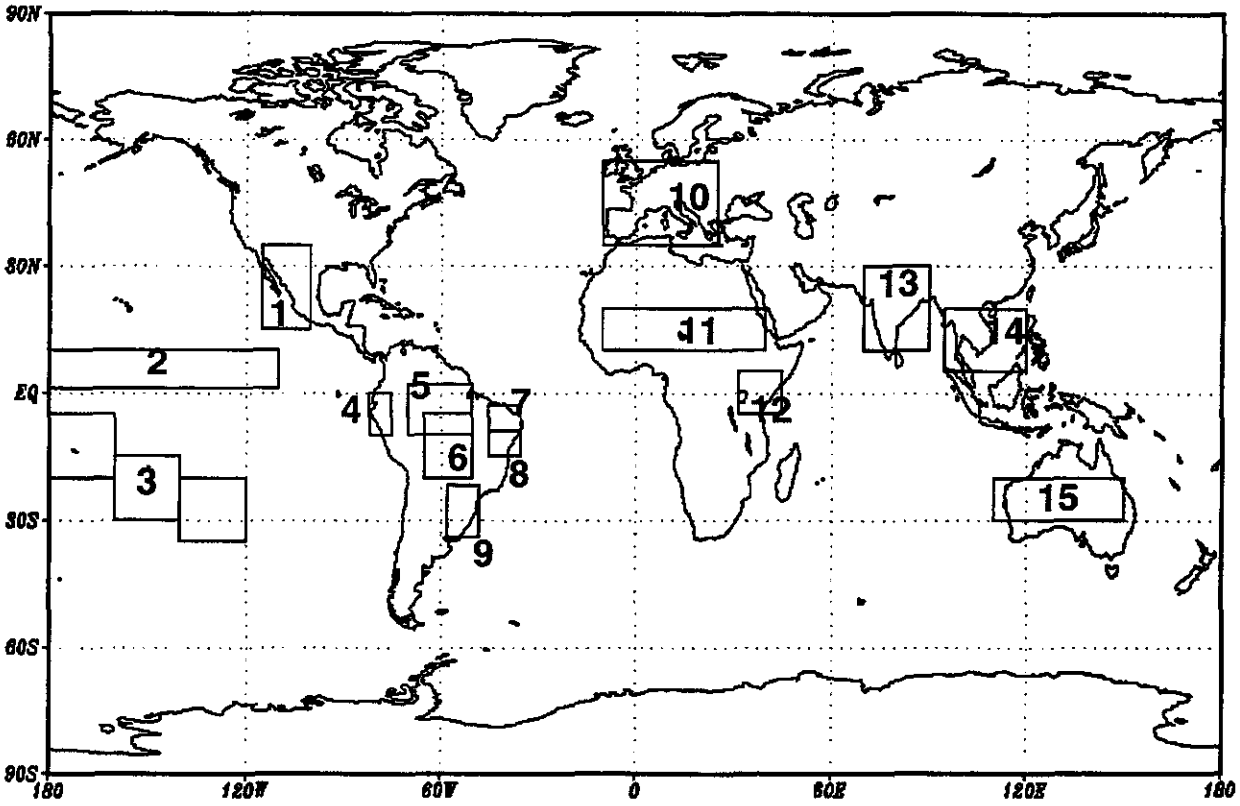


**1- North American Monsoon**
**2- Pacific ITCZ**
**3- SPCZ**
**4- Northwest Peru-Ecuador**
**5- Amazonia**
**6- South American Monsoon**
**7- North-Northeast Brazil**
**8- South-Northeast Brazil**
**9- Southern Brazil-Uruguay**
**10- Europe**
**11- Sahel**
**12- Eastern Africa**
**13- Indian region**
**14- Indonesia**
**15- Central Australia**

Fig. 4.1 - Selected continental and oceanic areas for regional studies.

# CHAPTER 5

# RESULTS

This section presents the highlights of the intercomparisons of the modeled and observed interannual variability of precipitation, and lower and upper level circulation and convection. We examine the statistical patterns of circulation, convection and rainfall fields for the 1982-91, either global or regional and also determine the skill of the model for several regions, using the BSS. Special analyses are performed for the two case studies, and some regional circulation and rainfall issues, such as the Amazon circulation and rainfall and the Indian-Southeast Asia monsoon are described in detail during those two contrasting situations.

## 5.1 INDICES OF INTERANNUAL VARIABILITY IN THE TROPICS AND SUBTROPICS

The tropical region shows a direct atmosphere response to SST anomalies, and thus shows an interannual variability associated with the extremes of ENSO. Previous work (Ward and Navarra, 1997) has indicated that in the tropics, unlike the extratropics, masking by natural internal variability generally is small. Therefore, in the following, we assess the model's ability to mimic the observed variability associated with the extremes of ENSO in the period 1982-91.

### 5.1.1 INDICES OF THE SOUTHERN OSCILLATON AND RELATED CIRCULATION, RAINFALL AND CONVECTION PATTERNS

Fig. 5.1a shows that the major interannual fluctuations, including the 1982/83 and 1986/87 El Niño, and the 1985/86 and 1988/89 La Niña events are well reproduced; with the model ensemble mean variation following closely the observed. The model SOI shows larger dispersion during the non-ENSO periods,

such as in 1984 and 1990. A systematic underestimation of the model sea level pressure nearby Tahiti (Cavalcanti et al., 2001) should not affect the calculation of SOI as it is calculated from anomalies.

Other indicators of the interannual variability in the tropical regions have also been calculated implemented, and expressed as normalized departures from climatology. These indices are the same used on the Climate Diagnostics Bulletin of NOAA/NCEP: (a) OLR averaged over the area 5 °N-5 °S/160 °E-160 °W (Fig. 5.1b) which is considered as indicator of tropical convection over central and west Pacific; (b) 200-hPa zonal wind anomaly index averaged over the area 5 °N-5 °S, 165 °W-110 °W (Fig. 5.1c) to detect the presence of easterly or westerly anomalies over the east-central Pacific; and (c) 500-hPa virtual temperature averaged over the latitude band 20 °N-20 °S (Fig. 5.1d), as an index of the warming (cooling) of the lower and middle atmosphere usually associated with the presence of El Niño (La Niña) in the equatorial Pacific. The 200 hPa index area was chosen based on a composite of El Niño episodes; the region is located between two upper-tropospheric anticyclonic anomaly centers. It also reflects the region were one normally finds equatorial westerlies associated with the mid-oceanic troughs. The 500 hPa virtual temperature index is a zonally averaged quantity, which reflects the intensity of either the warm or cold phase of ENSO (Kousky, personal communication).

The observed OLR index (Fig. 5.1b) exhibits negative departures during the 1982/83 and 1986/87 El Niño episodes, indicating enhanced tropical convection across the western and central Pacific, and reduced convection over Indonesia. Opposite pattern is deduced from the positive OLR index especially during the 1988/89 La Niña. The CPTEC/COLA AGCM depicts correctly this observed variability, with increased/reduced convection over western Pacific during the ENSO extremes.

The 200-hPa zonal wind index (Fig. 5.1c) shows observed intense easterly wind anomalies during the 1982/83 El Niño and the large westerly anomalies during the 1984/85 and 1988/89 La Niña, with the latter showing the largest anomalies. The model derived 200-hPa zonal wind index reproduced the observed easterly wind anomalies during the 1982/83 El Niño. The observed index is –2 times the standard deviation (approximately 10 $ms^{-1}$ below average) while the model shows an index of –1.5 times the standard deviation (approximately 7.5 $ms^{-1}$ below average). The major shortcoming of the simulation is that CPTEC/COLA AGCM 200-hPa zonal wind anomalies do not reproduce the largest westerly wind anomalies observed during 1988/89 La Niña, showing instead large easterly anomalies. The observed wind anomalies reach +2 times the standard deviation (up to 10 $ms^{-1}$ above the normal) and the model shows +0.5 times the standard deviation (barely above 3 $ms^{-1}$). The difference between observed and modeled wind anomalies during the 1984/85 La Niña was smaller than the 1988/89 event.

The 500-hPa virtual temperature anomaly in the tropical region (Fig. 5.1d) shows a much better agreement between model and observations. An observed relatively warmer atmospheric column is shown during the 1982/83 and the 1986/87 El Niño events, as well as during 1987/88 and 1989/90, while relatively cooler atmospheric column (represented as negative virtual temperature anomalies) is observed during 1984/85 and 1988/89 La Niña events. The AGCM estimates of the 500 hPa virtual temperature follow closely the observed anomalies, both in values and tendency.

In order to test the sensitivity of rainfall response to ENSO conditions and to illustrate the response of the CPTEC/COLA AGCM equatorial rainfall, convection and surface circulation, we have compared the east-west migration of the equatorial band of zonal circulation and rainfall belts from model and observations. Figs. 5.2 and 5.3 show the time-longitude equatorial (5 °S-5 °N) section of rainfall and 1000-hPa zonal winds from the CPTEC/COLA AGCM (Figs. 5.2a, 5.3a) and the respective verifications (Fig. 5.2b, 5.3b) from CMAP and NCEP.

The model simulates the eastward migration of the rainfall and zonal wind regions from western to central Pacific during the 1982/83 and 1986/87 El Niño events remarkably well. The model also reproduces quite well the observed double maximum of rainfall over the western Pacific (140-160 °E) and over the Indian Ocean (80-100 °E). On the other hand, Figs. 5.2a illustrates a generic problem of the phase locking of spurious rainfall to the topography of the maritime continent (at 100 °E, 120 °E, and 140 °E) and the Andes around 80 °W. This is also depicted in both model OLR sections (not shown).

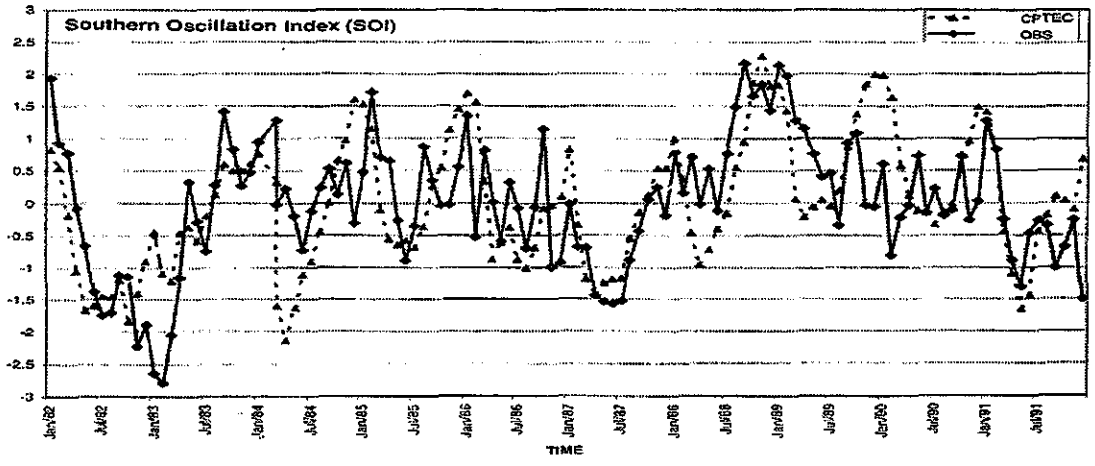


(A)

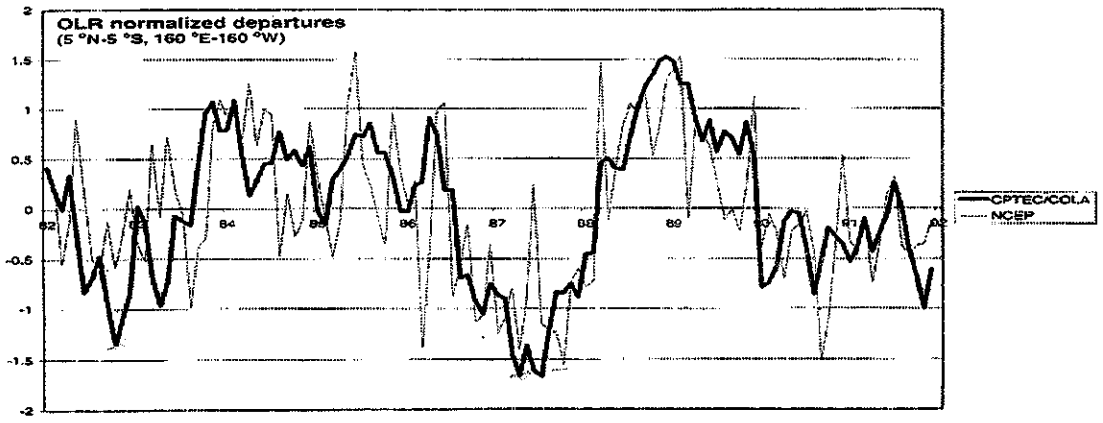


(B)

Fig. 5.1 - Indices of interannual variability for the tropical region. (a) Southern Oscillation Index calculated with observed sea level pressure at Tahiti and Darwin for a 10-year period 1982-91 plotted as solid line. The ensemble of the 9 integrations of the CPTEC/COLA GCM is shown as broken line. (b) Outgoing longwave radiation normalized departure index averaged over the area 5 $^{O}$N-5 $^{O}$S, 160 $^{O}$E-160 $^{O}$W. (c) 200 h-Pa zonal wind normalized departure index averaged over the area 5 $^{O}$N-5 $^{O}$S, 165 $^{O}$E-110 $^{O}$W. (d) 500 h-Pa virtual air temperature normalized departure index averaged over the latitude band 20 $^{O}$N-20 $^{O}$S. Observations are shown as thin line, and the ensemble of the 9 integrations of the CPTEC/COLA AGCM is shown as full line (continua)

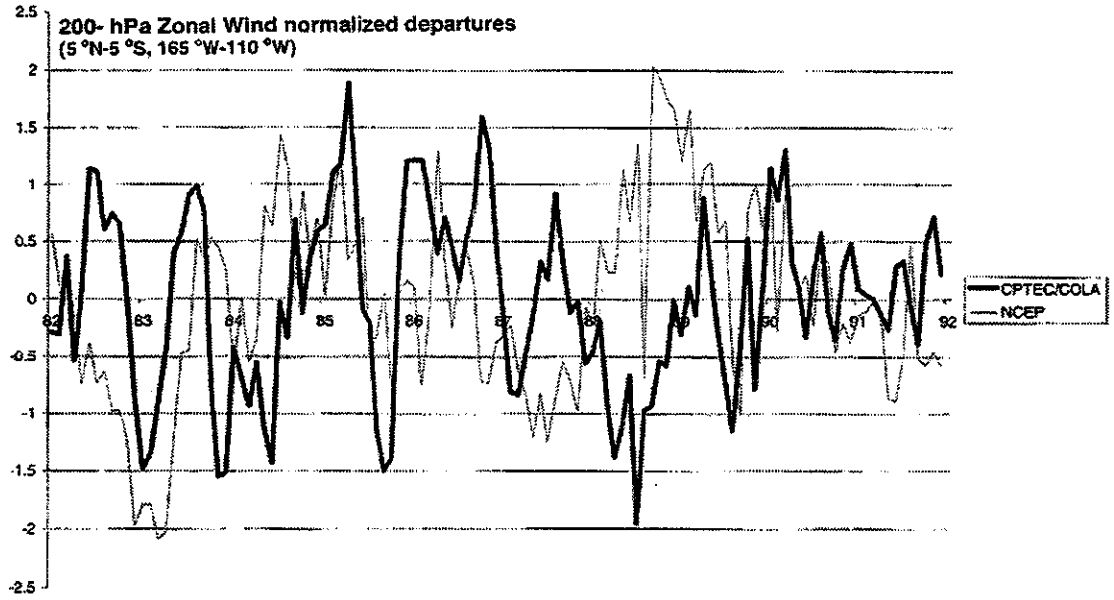


(C)

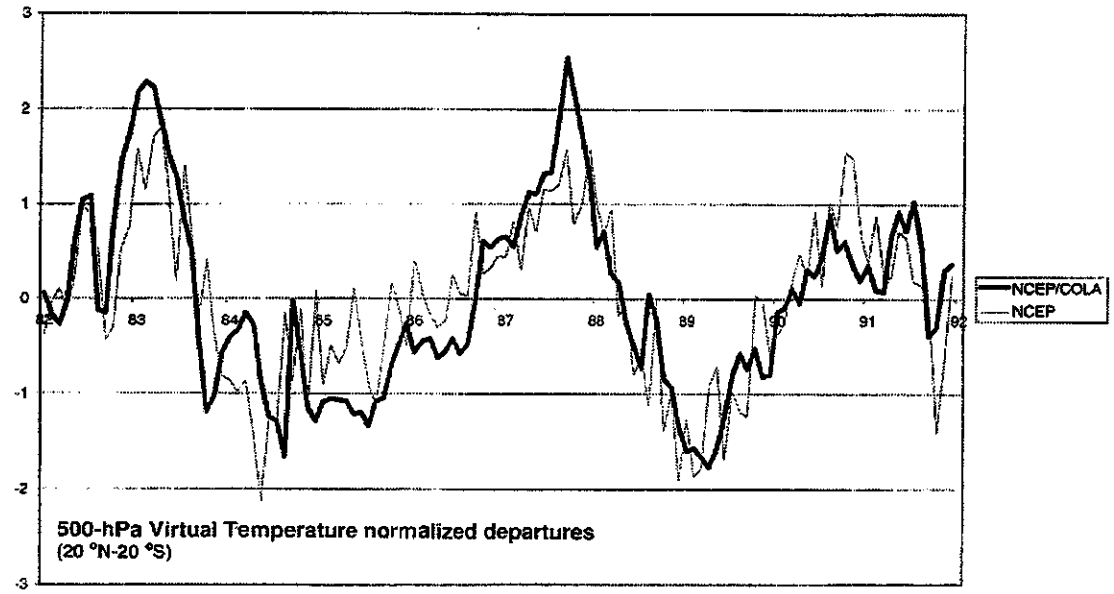


(D)

Fig. 5.1- (conclusão)

In this regard, Lau et al. (1996) acknowledge the artificial anchoring of precipitation to topographic features in the maritime continent as a generic problem in many AMIP models. The model shows the observed reduced convection and rainfall in

Amazonia and Northeast Brazil during the 1982/83 and 1986/87 El Niño events, and the larger rainfall and convection over the same regions in 1984 and 1985. Fig 5.3a, b show the enhanced easterly wind anomalies over the central and eastern Pacific during the 1982/83 and 1986/87 El Niño events, as well as the large westerly wind anomalies during the 1988/89 La Niña.

In sum, we can say that the observed and simulated rainfall and circulation indices of the SO show a close agreement, and the observed shifts in tropical and equatorial convection, circulation and rainfall associated with variations in the observed SO index are also well simulated by the CPTEC/COLA AGCM.

### 5.1.2 POSITION AND INTENSITY OF THE BOLIVIAN AND TIBETAN UPPER-TROPOSPHERIC ANTICYCLONES

The Andes and the Himalayas are an elevated heat source that generates solenoidal upslope circulations in summer. These circulations are most active in the afternoon, when they promote convection over the mountain peaks and slopes. The South American Altiplano is centered on Bolivia, northern Chile, and Peru. An anticyclonic circulation referred to as the "Bolivian high" during the southern summer commonly surmounts it. Dynamic and thermodynamic foundations of the Bolivian high are subjects of active research, (e.g. Lenters and Cook, 1995, 1997,1999; Figueroa et al., 1995; Garreaud, 1999). On the other hand, the mountainous region of the Himalayas influences the atmospheric response to the solar heating gradient by elevating the land heating of the atmosphere to the middle atmosphere, this heating is primarily responsible for the build-up of an upper-level high over the central Asian mountain massifs, and this anticyclonic circulation is referred as the "Tibetan High" during the northern summer. The annual cycle of these two centers and their migrations are explained in Hastenrath (1996, p. 202-203).

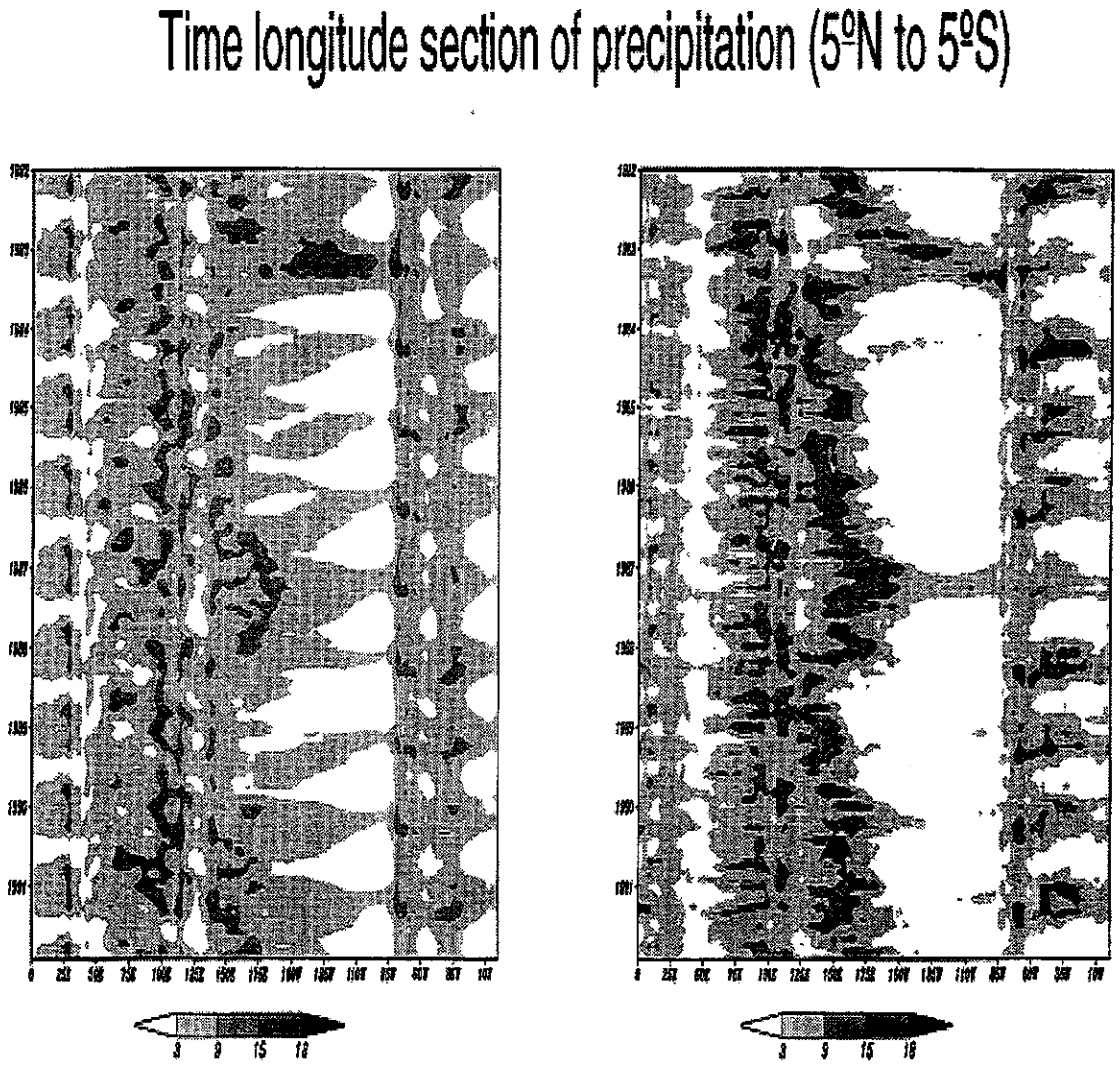


Fig. 5.2 - Time-longitude section of precipitation averaged over 5 $^{O}$N-5 $^{O}$S for (A) CPTEC/COLA AGCM, and (B) the CMAP rainfall observations.

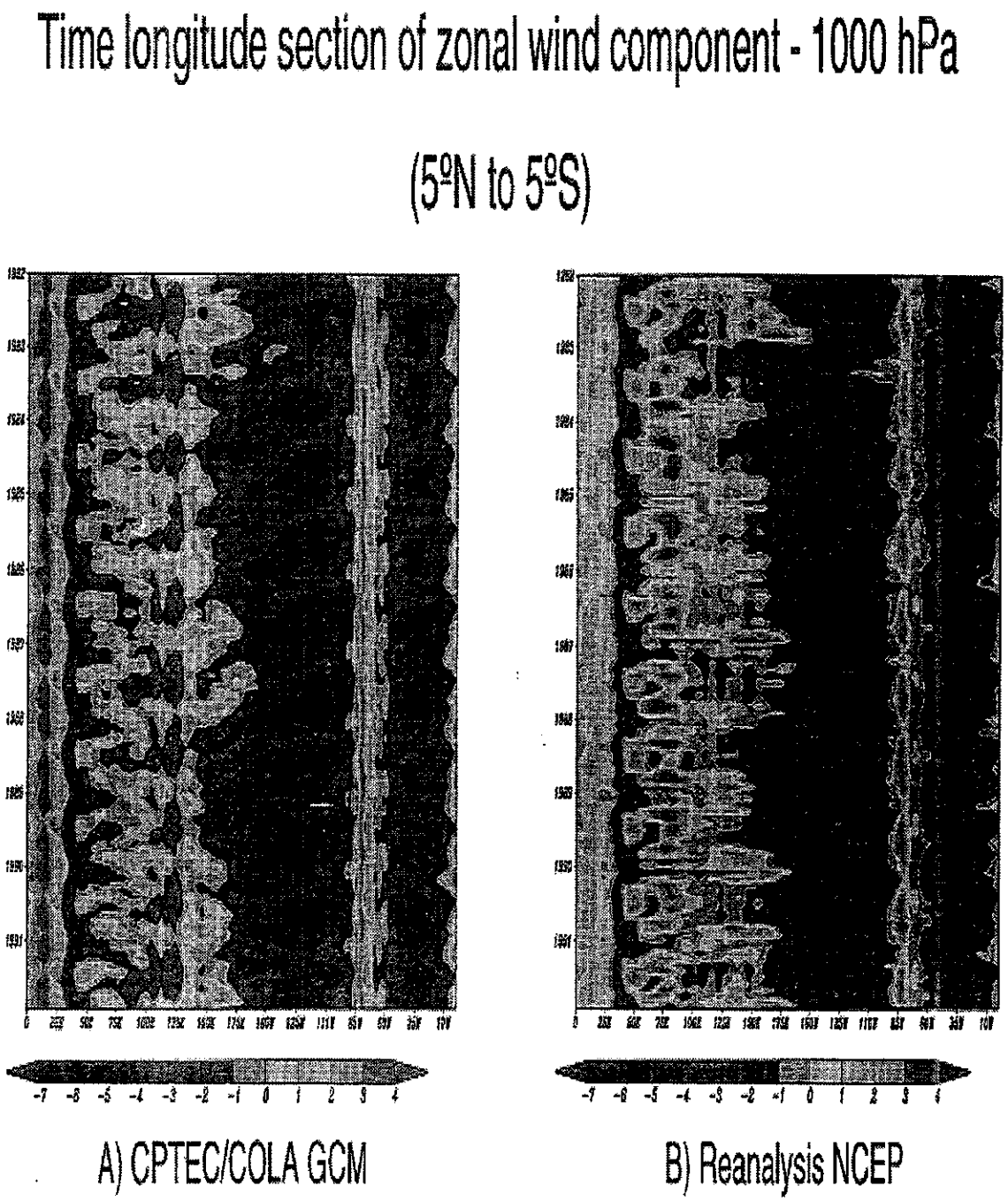


Fig. 5.3 - Time-longitude section of 1000 hPa zonal wind averaged over 5 $^{O}$N-5 $^{O}$S for (A) CPTEC/COLA AGCM, and (B) the NCEP/NCAR reanalyses.

Since the Bolivian and Tibetan Highs are components of the monsoon systems in South America and India, it is of great importance to investigate if the model

reproduces these two components of the monsoon systems, their seasonal and interannual variability, that may led to a successful forecasting of the strength of a monsoon season on those regions. Observations and model simulation show the upper tropospheric Bolivian High during the DJF season as the South American monsoon system develops (Fig. 5.4).

Fig. 5.4 shows the mean position of the Bolivian high during the DJF summertime season, from the NCEP/NCAR reanalysis and from the CPTEC/COLA AGCM ensemble mean. The observed center of the high is established near 17 °S, 62 °W, while the mean modeled position is shifted southwestward from the observed position near 19.5 °S, 68 °W.

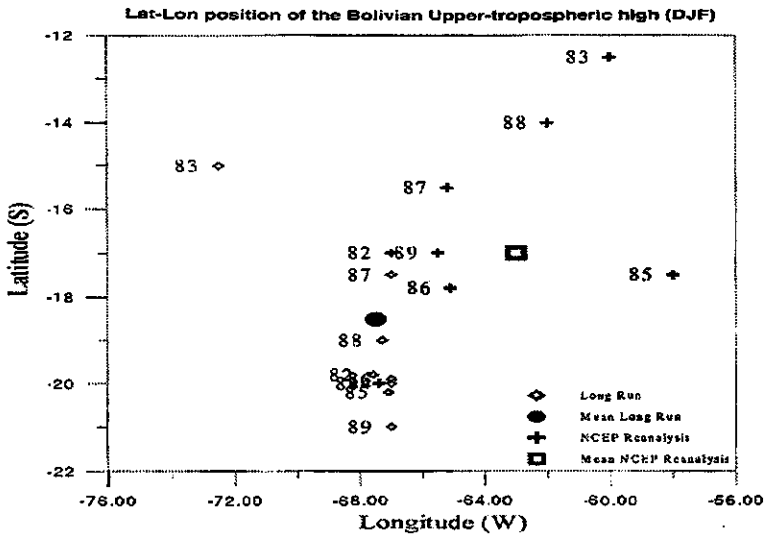


Fig. 5.4 - Mean position of the upper-tropospheric anticyclone in South America during summertime (DJF) for the period 1982-91, as produced by the ensemble mean of the CPTEC/COLA AGCM (diamonds) and from the NCEP/NCAR reanalyses (plus sign). The mean modeled position is indicated with a circle, and the mean observed position is indicated by a square.

Fig. 5.4 shows that the Bolivian High is also affected by the tropical Pacific forcing, since the ENSO SST warming determines changes to its interannual position and

intensity, becoming displaced northward during El Niño years and southward displaced during La Niña events. The differences between the position and intensity of the observed and modeled Bolivian High implies systematic differences in the position of the upper-level cold trough off the east coast of Brazil, and the South Atlantic Convergence Zone (SACZ) and in the development of the monsoon system that reaches their seasonal maximum just prior to the onset of the rains.

These differences in the mean observed and modeled position of the Bolivian High also can be linked to an underestimation of convection and rainfall in Amazonia, especially in northern and central region. In fact, when it is weak and located further to the west, as depicted systematically by the CPTEC/COLA AGCM, there is a tendency for an intensification and a southward extension of the model convection over the SACZ area and inhibition of convection over the Bolivian Plateau. In that case, successive frontal systems penetrate into tropical latitudes and remain quasi-stationary over southeastern Brazil, and they contribute to drain moisture from the Amazon into the SACZ, inhibiting a southward flow of moisture on the eastern slope of the Andes.

The model SACZ tends to be too strong and southward displaced, as compared to observations (Cavalcanti et al., 2001), and this is especially observed on the southernmost section nearby the South Atlantic, while tends to be weak on the northwest section on the border of Amazonia and the South American monsoon region. This can be related to the mechanisms of formation and maintenance of the Bolivian High as produced by the model, where an apparent underestimation of latent heat in the Amazon region and in the Bolivian plateau may be affecting the regional circulation, including the southwestward shifting of the Bolivian High, and the shrinking of the upper-level trough over Northeast.

For the Tibetan High, (Fig. 5.5), the mean modeled and observed positions are in agreement, with the model anticyclone located approximately at 27.8 °N, 92 °E, which is 0.3 degrees to the north of the observed mean position derived from the

NCEP/NCAR reanalyses (27.5 °N, 92 °E). This apparent good performance of the model in depicting the observed position of the Tibetan High does not necessarily mean that rainfall over this region is going to be well represented in terms of distribution and variability, as is discussed in the following sections. Year-to-year variability of the modeled and observed position of the center of the Tibetan High and the Indian monsoon system have been reported as being dependent not only on SST anomalies in the Pacific-Indian Ocean, but also on the seasonal and interannual variations of soil moisture and the snow cover over Eurasia, indicating the importance of land surface processes on the following Indian summer monsoon season (Webster et al., 1998; Matsuyama and Masuda, 1998).

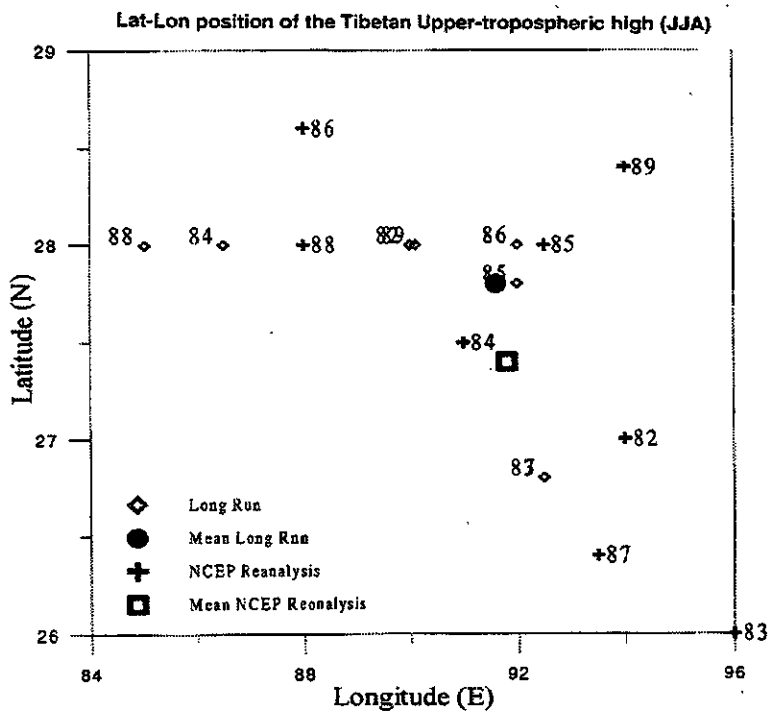


Fig. 5.5 - Mean position of the upper-tropospheric anticyclone in the Tibet region during summertime (JJA) for the period 1982-91, as produced by the ensemble mean of the CPTEC/COLA AGCM (diamonds) and from the NCEP/NCAR reanalyses (plus sign). The mean modeled position is indicated with a circle, and the mean observed position is indicated by a square.

## 5.2 PRECIPITATION

### 5.2.1 GLOBAL FEATURES

Table 5.1 shows mean and deviation of the modeled and observed precipitation for the global, hemispheric, tropical and equatorial bands, for both ocean and land. The rainfall amounts during the extremes of 1982/83 El Niño and 1988/89 La Niña are also given in the table. The observed mean global rainfall from 1982-91 CMAP is 2.7 mm $day^{-1}$; while the CPTEC/COLA AGCM produces an annual global mean (ocean and land) precipitation of 3.5 mm $day^{-1}$, and exhibits an exhibits a 1982-91 standard deviation of 0.1 mm $day^{-1}$. The CPTEC/COLA AGCM land-only 1982-91 precipitations is 2.5 mm $day^{-1}$ with a standard deviation of 0.11 mm $day^{-1}$. For comparison, the study by Lau et al. (1996) the observed model ensemble from the 1979-88 AMIP AGCMs gives 2.8 mm $day^{-1}$, with a standard deviation 0.5 mm $day^{-1}$. In their study, the COLA GCM, from where the CPTEC/COLA AGCM is derived, compares quite well (less than 1 standard deviation) with an annual mean precipitation of 2.8 mm $day^{-1}$ over land.

In general, the model tends to overestimate the observed rainfall at global and hemispheric scales. In contrast, this tendency is less pronounced in equatorial latitudes as compared to higher latitudes. While the CMAP shows a 1982-91 average of 5.5 mm $day^{-1}$ in the equatorial band, the model shows 4.8 mm $day^{-1}$. During 1982/83 El Niño both model and observations show more rainfall in the equatorial band, as compared to 1988/89 La Niña, and in general for both Northern and Southern hemisphere the model rainfall estimates are larger than observations, both for the entire period 1982-91 and for the two extremes of the SO in 1982/83 and 1988/89 (Table 5.1).

**TABLE 5.1: COMPARISON BETWEEN GLOBAL AVERAGES OF LAND AND SURFACE PRECIPITATION FOR OBSERVED (CMAP) AND MODELED (MEAN OF THE 9-MEMBERS ENSEMBLE), FOR LATITUDINAL BANDS: GLOBAL, NH (NORTHERN HEMISPHERE 0- $^{o}$90 N), SH (SOUTHERN HEMISPHERE 0-90 $^{o}$S), TROPICS (25 $^{o}$N-25 $^{o}$S) AND EQUATOR (5 $^{o}$N-5 $^{o}$S). THE BASE PERIOD IS 1982-91. VALUES FOR EL NIÑO 1982/83 WERE FROM DECEMBER 1982 TO NOVEMBER 1983, AND FOR LA NIÑA 1988/89 WERE FROM DECEMBER 1988 TO NOVEMBER 1989. UNITS ARE IN mm day$^{-1}$. THE STANDARD DEVIATION IS SHOWN BETWEEN BRACKETS.**

| Data set/year | Global | NH | SH | Tropics | Equator |
|---|---|---|---|---|---|
| CPTEC COLA AGCM (1982-91 mean) | 3.5 [0.1] | 3.5 [0.4] | 3.5 [0.4] | 4.7 [0.1] | 4.8 [0.8] |
| CMAP (1982-91 mean) | 2.7 [0.1] | 2.7 [0.6] | 2.6 [0.5] | 3.6 [0.2] | 5.1 [0.9] |
| CPTEC/COLA AGCM (El Niño 1982/83) | 3.5 | 3.4 | 3.6 | 4.4 | 5.5 |
| CMAP (El Niño 1982/83) | 2.7 | 2.6 | 2.9 | 3.7 | 5.6 |
| CPTEC/COLA AGCM (La Niña 1988/89) | 3.5 | 3.5 | 3.6 | 4.7 | 4.7 |
| CMAP (La Niña 1988/89) | 2.6 | 2.7 | 2.8 | 3.6 | 4.5 |

### 5.2.2 INTERANNUAL VARIABILITY: GLOBAL, HEMISPHERIC, TROPICAL AND EQUATORIAL

As a test of the sensitivity of the rainfall response to SST and to ENSO conditions, and to illustrate some of the problems in tropical rainfall simulation by the CPTEC/COLA AGCM, Fig. 5.6a-e shows time series of area-averaged precipitation for different latitudinal bands. For both Northern and Southern Hemispheres (Fig. 5.6a, b) there is a good agreement between model and the CMAP observations, with a realistic model annual cycle. There is some scatter among members of the ensemble especially during the rainy season, due mainly to the different rainfall regimes and rain producing mechanisms in several climatic regions of both hemispheres, such as tropical rainfall belts and the storm tracks at midlatitudes. In both northern and southern tropics (Fig. 5.6c and d) the model captures remarkably well the annual cycle and the amount.

For equatorial latitudes (5 $^{o}$N-5 $^{o}$S, Fig. 5.6e) the agreement between model and observations is quite good, both in amount of rainfall and the annual cycle. This region includes most of the West Pacific warm pool, and the eastern Pacific-northwest coast of South America, and the forcing due to large positive SST anomalies is reflected in the fact that the model reproduces the observed large amounts of rainfall in the region during the 1982/83 and 1986/87 El Niño events, with extreme large amount of rainfall in the East Pacific contrasting with reduced rainfall over the West Pacific.

Based on the normalized rainfall departures shown in Fig. 5.6 and the actual rainfall amounts (Table 5.1), it is observed that in general the model ensemble depicts quite well the annual cycle, even though there is a tendency for the model to overestimate rainfall. For the northern and southern tropics, the model reproduces the observed annual cycle of rainfall. The tendency to overestimate rainfall still holds, but the difference between model and observations is less than

10% during the respective rainy season. In the equatorial region, the model captures quite well both the variability and the observed rainfall amounts.

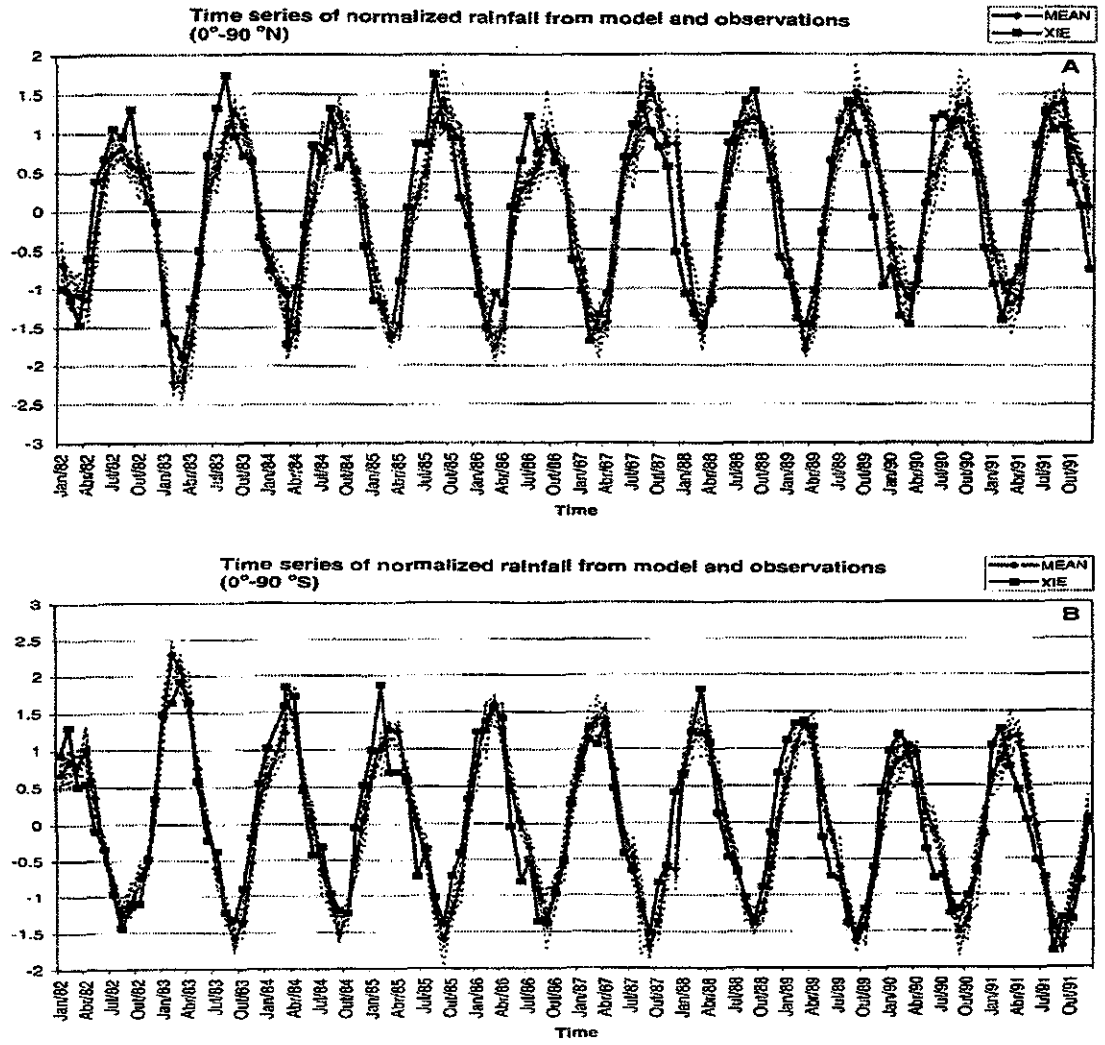


Fig. 5.6 - Time series of normalized departures of area-averaged precipitation for the ensemble mean of the CPTEC/COLA AGCM (full line with diamonds) and from the CMAP data (full line with squares). The 9 individual integrations are presented as broken lines. (a) Northern hemisphere (0-90 $^{O}$N), (b) Southern hemisphere (0-90 $^{O}$S), (c) Northern tropics (25 $^{O}$N-0), (d) Southern tropics (0-25 $^{O}$S), (e) Equatorial region (5 $^{O}$N-5 $^{O}$S). (continua)

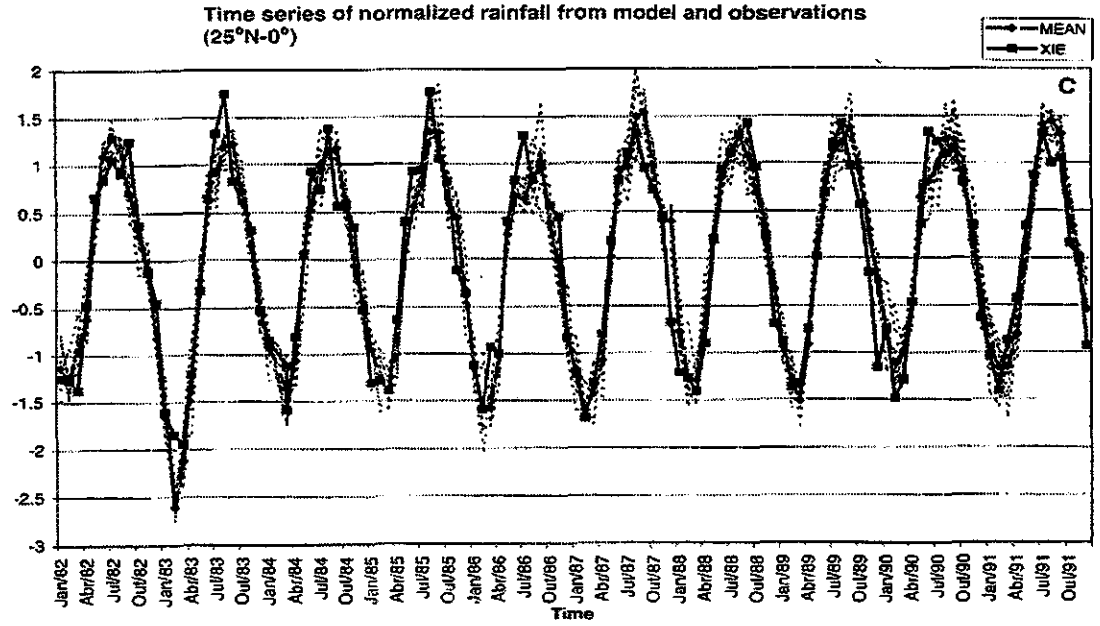


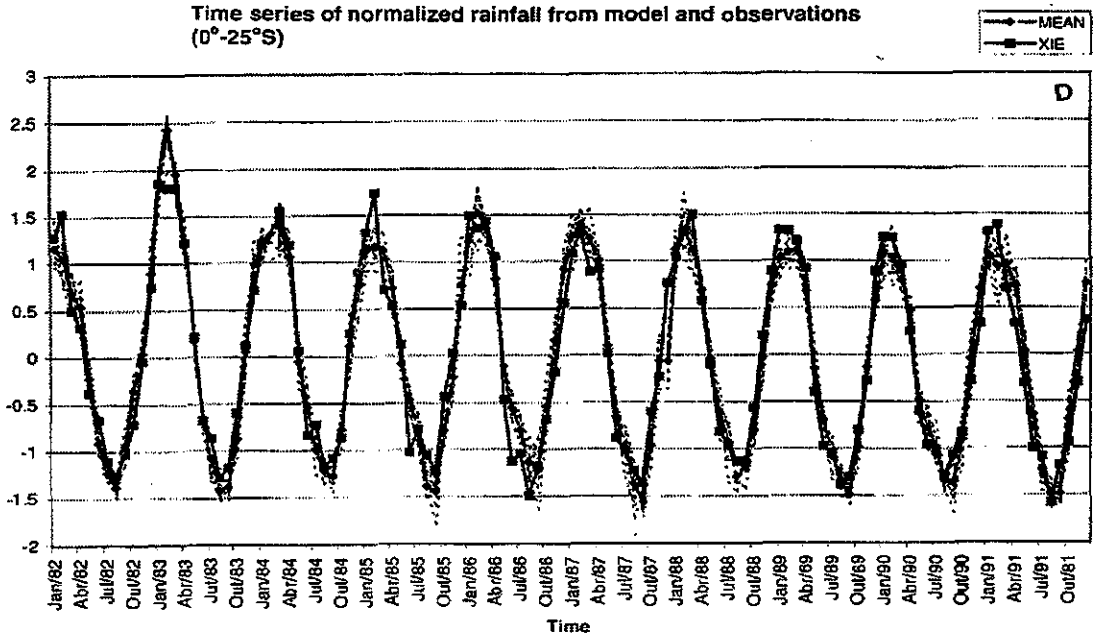


Fig. 5.6 -

(continua)

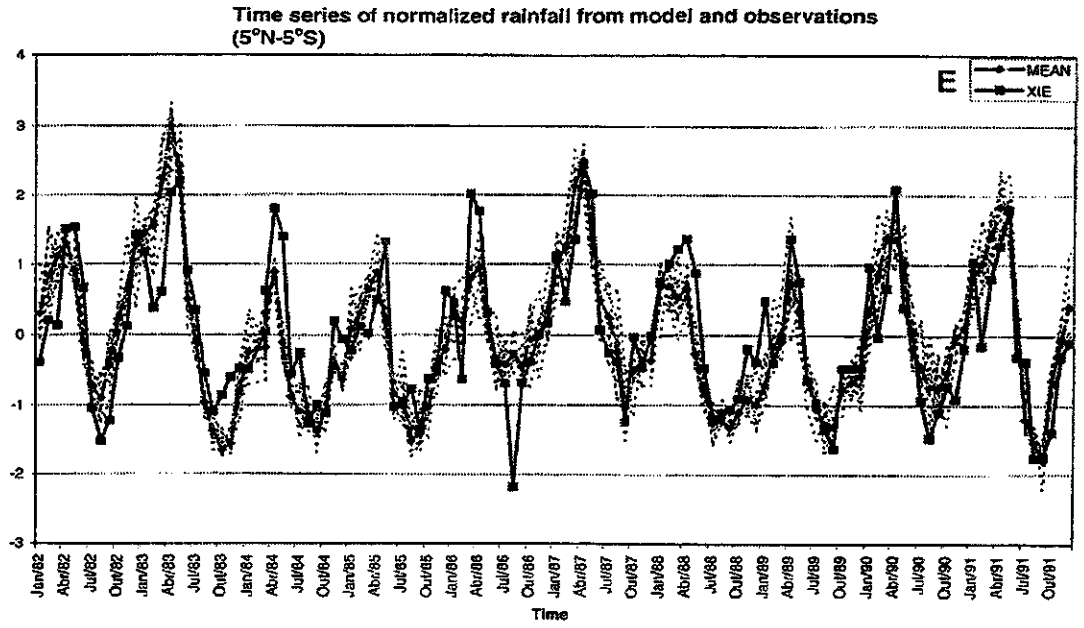


Fig. 5.6 - (conclusão)

### 5.2.3 ZONAL MEANS

The zonal mean profiles of observed and modeled precipitation are displayed for DJF 1982/83, JJA 1983 (Fig. 5.7a, b), DJF 1988/89 and JJA 1989 (Fig. 5.7c, d), representative of the two extremes of ENSO. Each figure shows the mean and the individual members of the ensemble and the CMAP observed rainfall for the respective case. In general the model simulates the overall latitudinal structure of the observed estimates, including the equatorial maximum and the secondary maximum in mid-latitudes for both hemispheres.

For the DJF 1982/83 case, Fig. 5.7a shows a maximum of 7.5 mm $day^{-1}$ at approximately 0-7 °S, while the average for the season reaches similar amount. The model depicts quite well this maximum and its latitudinal location, and the spread among members of the ensemble is not large. However, the model seems to produce a second maximum of approximately 6 mm $day^{-1}$ at 5 °N, which is not depicted on the CMAP data.

During 1982/83, the model produces mid-latitude peaks at 35 °N and 45 °S approximately, smaller than for the 1982-91 mean, and a relative minimum of rainfall of 6 mm $day^{-1}$at around the equator, between the maximum of 7.5 and 6.5 mm $day^{-1}$, which is not depicted by the CMAP observations for DJF 1982/83. The JJA 1983 zonal rainfall distribution (Fig. 5.7b) is not much different than the climatology (Cavalcanti et al., 2001).

During the 1988/89 La Niña (Fig. 5.7a, b), the agreement seen as in the 1982/83 situation is not observed, and even though during DJF the model reproduces the location of the observed zonal tropical rainfall peak, they are overestimated and shifted few degrees poleward. This indicates that in fact, the tropical atmosphere is very sensitive to strong warming over the equatorial Pacific, more sensitive than to a cooling on the same region of the Pacific.

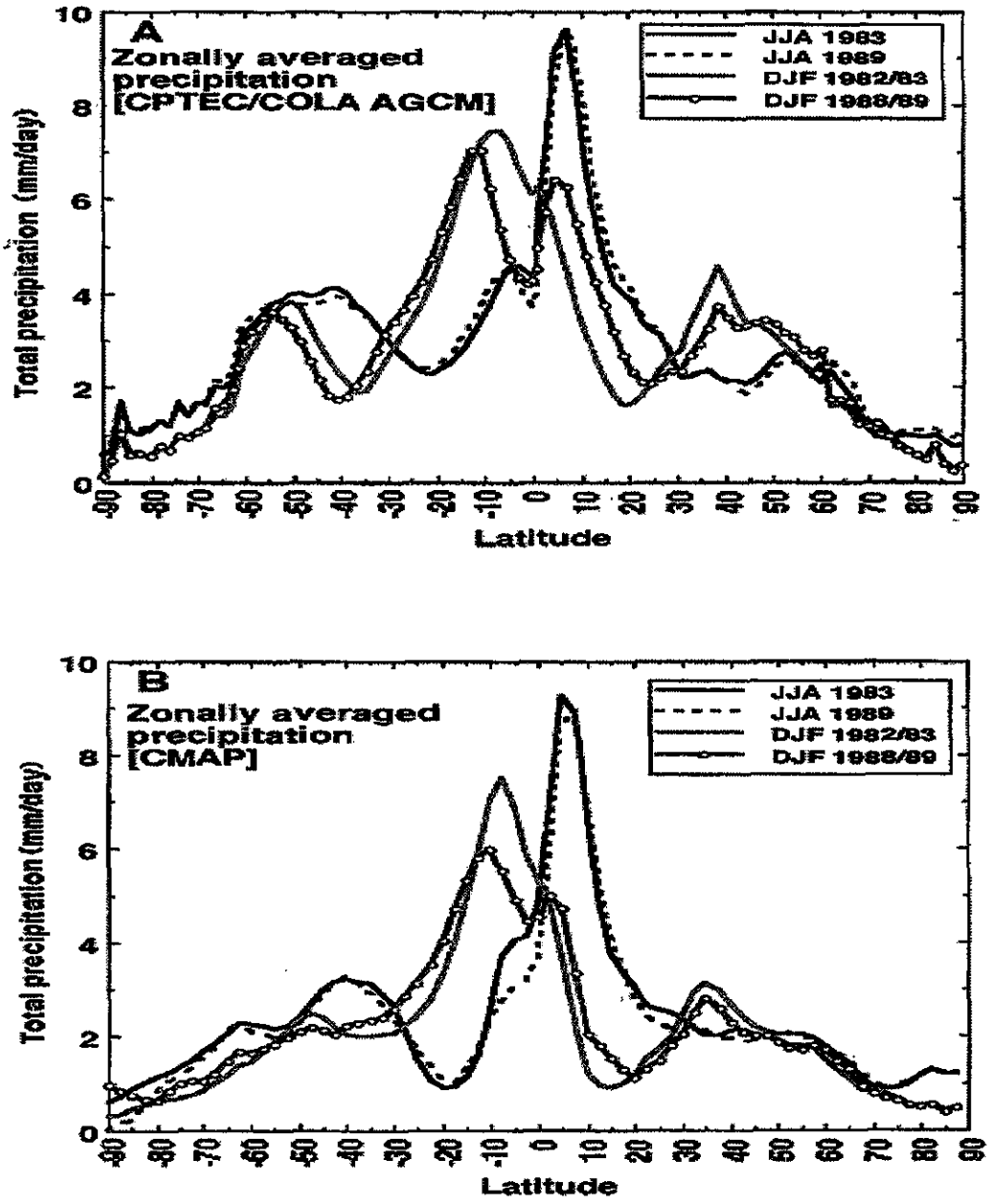


Fig. 5.7 - Zonal mean precipitation from the 9 individual integrations (broken lines), the ensemble mean of the (a) CPTEC/COLA AGCM , and (b) CMAP. Lines represent the DJF 1982/83, and DJF 1988/89 as well as JJA 1983 and JJA 1989.

### 5.2.4 REGIONAL STUDIES

Previous experiences on interannual variations in Northeast Brazil by Sperber and Palmer (1996) have shown that rainfall in this region is well captured by atmospheric models with prescribed SST. This is also the case for the South American monsoon (Robertson et al., 1999) and the West Africa monsoon (Rowel at al., 1995; Semazzi et al., 1996; Goddard and Graham, 1999). The CPTEC/COLA AGCM precipitation in India is less well simulated. However the models show better skill in reproducing the interannual variability of a wind shear index over the Indian summer monsoon region indicating that the model exhibit greater fidelity in capturing large-scale dynamic fluctuations than the regional scale rainfall variations.

In the following, we assess the ability of the model to simulate interannual rainfall variability over some regions of the planet in response to anomalous SST forcing. To do this, rainfall indices were computed as deviations from the mean climatology from model and observations for the regions shown in Fig. 4.1. Climate variability of some of these regions is linked to the interannual variability associated with the extremes of the Southern Oscillation (Fig. 5.8). Table 5.2 shows the mean and standard deviations of the observed and modeled rainfall in some of these regions, for their respective rainy seasons.

**TABLE 5.2 - MEAN AND STANDARD DEVIATION (STD) OF OBSERVED RAINFALL (FROM CMAP) AND MODELED RAINFALL (mm day$^{-1}$) AT SEVERAL REGIONS SHOW IN FIG. 4.1. THE SECOND COLUMN SHOWS THE MEAN OF THE RAINY SEASON AT EACH REGION. THE BASE PERIOD IS 1982-91, AND TABLE SHOWS THE MEAN OF THE MEMBERS OF THE ENSEMBLE.**

| Region | Rainy Season | Observations | | Model | |
|---|---|---|---|---|---|
| | | Mean | STD | Mean | STD |
| Pacific ITCZ | JASOND | 6.20 | 0.99 | 6.96 | 1.17 |
| SPCZ | DJF | 19.56 | 1.54 | 19.9 | 1.29 |
| Northwest Peru-Ecuador | DJF | 3.70 | 0.65 | 5.00 | 0.92 |
| Amazonia | MAM | 7.87 | 0.62 | 5.86 | 0.33 |
| N. Northeast Brazil | MAM | 5.94 | 2.12 | 8.01 | 1.49 |
| S. Northeast Brazil | MAM | 3.82 | 0.85 | 8.24 | 1.91 |
| S. Brazil-Uruguay | JJAS | 3.26 | 0.61 | 2.21 | 0.27 |
| S. American monsoon | DJF | 2.32 | 0.22 | 2.49 | 0.15 |
| N. American monsoon | JJA | 3.42 | 0.74 | 3.80 | 0.54 |
| Europe | MJA | 1.36 | 0.12 | 1.70 | 0.12 |
| Sahel | JAS | 3.44 | 0.44 | 5.23 | 0.41 |
| Eastern Africa | MJJAS | 1.37 | 0.29 | 2.64 | 0.20 |
| India | JJAS | 6.68 | 0.59 | 6.42 | 0.53 |
| Indonesia | JJAS | 9.37 | 0.68 | 6.34 | 0.96 |
| Central Australia | JFM | 1.31 | 0.52 | 1.52 | 0.32 |

For Northeast Brazil (Fig. 5.8a, b), the major interannual fluctuations, including the 1982/83, 1986/87 El Niño, and the 1988/89 La Niña, as well as the anomalously wet year of 1985, are well simulated by the model both on its northern and southern sections of the region (Fig. 5.8a, b). The dispersion among members of

the ensemble for the MAM peak of the rainy season is not as large as in other regions such as southeastern Brazil. In fact, in southern Brazil-Uruguay (Fig. 5.8c) the intra-member model spread is larger than 2 standard deviations from the ensemble mean. The model captures well the positive rainfall anomalies during boreal fall 1983, and with less intensity, the negative departures during the 1988/89 La Niña. Similar explanation is valid for the Pacific ITCZ (Fig. 5.8d), where the model ensemble rainfall compares remarkably well with the observations.

For the American monsoon systems (Fig 5.8e, f), modeled and observed rainfall amounts are in good agreement (Table 5.3). However, there is a large inter-member spread in the South American monsoon area (Fig. 5.8e), as compared to the North American monsoon (Fig. 5.8f), and the large positive or negative rainfall anomalies shown in the observations are not reproduced by the model.

For the Amazon basin (Fig. 5.8g), the model interannual variability resembles very well the observed variability, with lower rainfall during the 1982/83 and 1986/87 El Niño events, and relatively abundant rainfall during the 1988/89 La Niña episode. However, there is a tendency for underestimation of the rainfall amount for the Amazon basin in the CPTEC/COLA AGCM (See Table 5.1). This indicates that the model does not reproduce the organized large-scale convection over most of central-northern Amazonia and the intense low-level moisture convergence during the peak of the rainy season from January through March. This is linked to the reported tendency of the model to underestimate convergence of the trade winds convection and rainfall in that area.

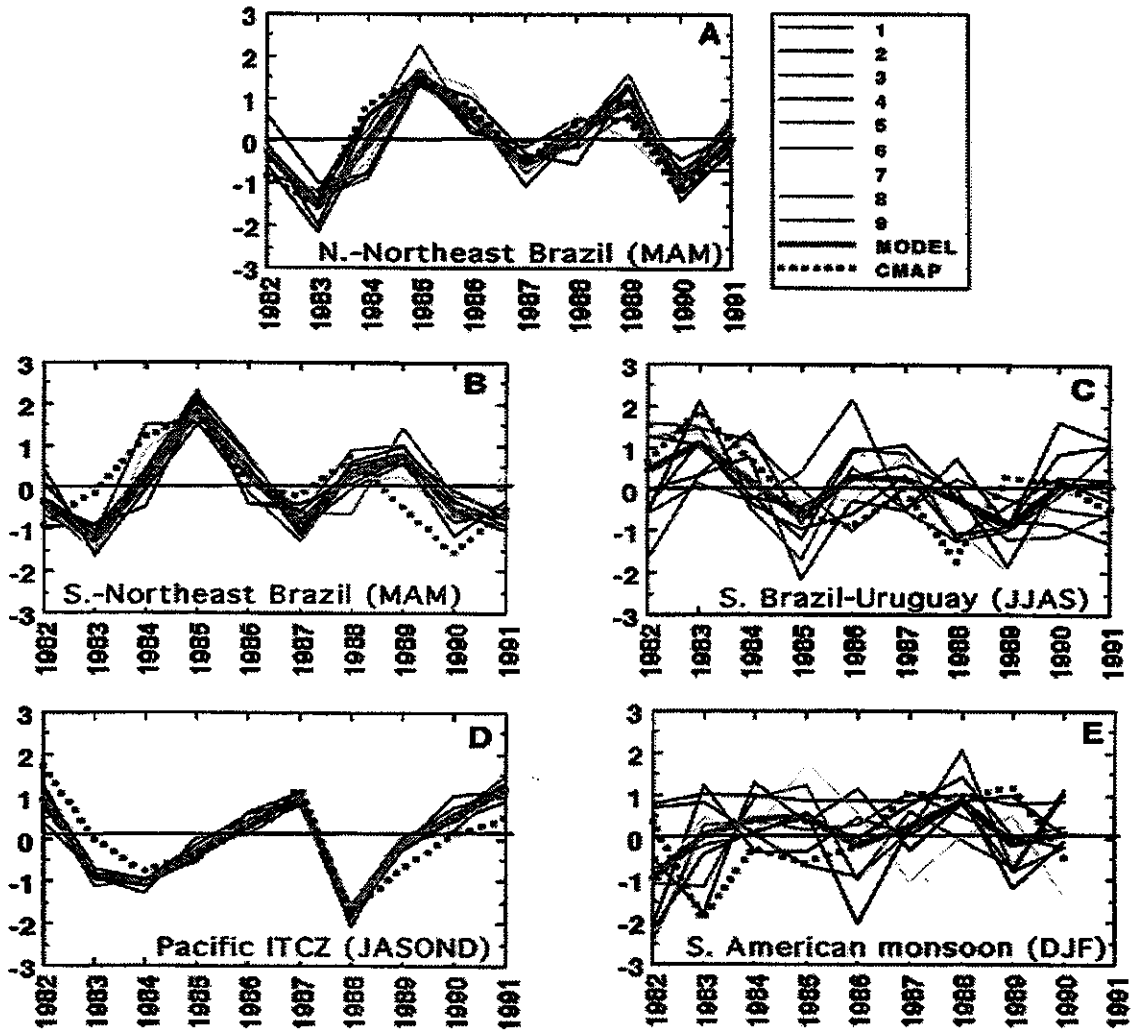


Fig. 5.8 - Time series of rainfall anomaly during the peak of the rainy season in several areas depicted in Figure 4.1. Thin solid lines represent the 9 individual integrations, a thick solid line represents the ensemble mean of the CPTEC/COLA AGCM, and observations from CMAP data are represented by thick broke line. (a) North- Northeast Brazil (MAM), (b) South-Northeast Brazil (MAM), (c) Southern Brazil-Uruguay (JJA), (d) Pacific ITCZ (JASOND), (e) South American monsoon (DJF), (f) North American monsoon (JJA), (g) Amazonia (MAM), (h) Indian region (JJAS), (i) Eastern Africa (JJA), (j) Sahel (JJA), (k) Northwest Peru-Ecuador (DJF).

(continua)

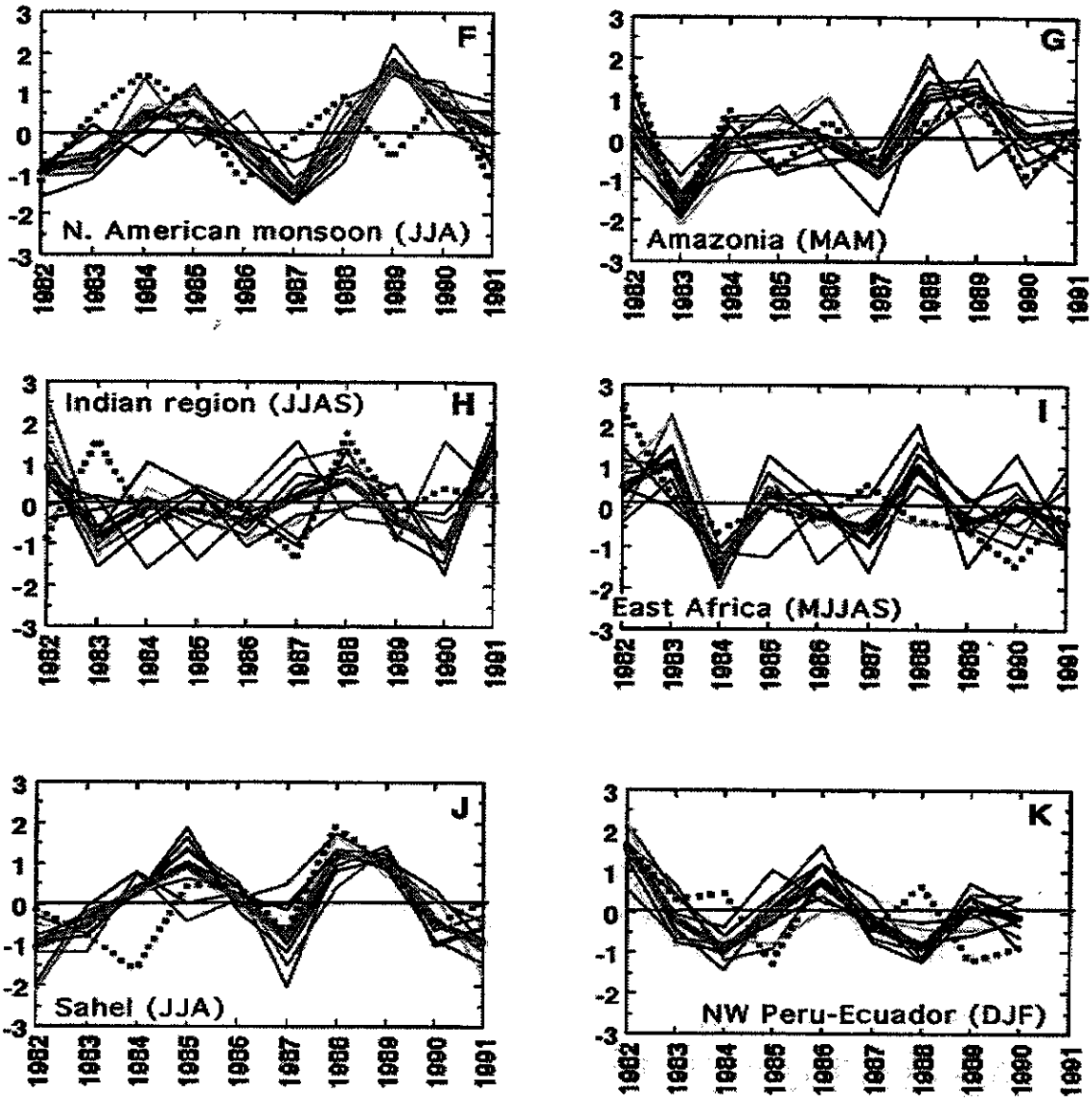


Fig. 5.8 - (conclusão)

This tendency for underestimation of rainfall in the Amazon region has also been observed in other global climate models and also for regions such as Indonesia and equatorial Africa (GISS AGCM, Hansen et al., 1983; Marengo and Druyan, 1994). These two models underwent modifications in both physical and dynamical formulations for radiation, land-surface and convection processes (Marengo and Druyan, 1994; Marengo et al., 1994; Kiehl et al., 1998), and the improved versions

produce increased rainfall, which are much closer to the observed rainfall in Amazonia and other regions of the tropics.

Over the Indian region there is large spread among members (Fig. 5.8h), and a tendency, which is consistent with the large spread of simulations of Indian monsoon rains from 8 models for AMIP (Magaña and Webster, 1998). The modeled interannual variability exhibits negative rainfall departures (Fig. 5.8h) in 1983, 1986 and 1990, with a large spread among members As indicted Webster (1998), the main differences between the impacts of El Niño on the monsoon in India and the Americas are function of phase. El Niño years in the Pacific are often followed by drought years in the Indian region, as in 1983, indicating weak monsoons. For the 1983 El Niño year, the CMAP-derived positive rainfall anomaly contrasts with the modeled negative rainfall departure. This tendency contrasts well with the weak Indian monsoons during El Niño produced for several other climate models (Latif et al., 1999). The observed rainfall anomalies in our analyses were based on CMAP from 1982-91 only. For comparison, the June-September all-India rainfall index of 1958-97 from Sperber et al. (1999a) exhibits an observed interannual variability with larger positive rainfall anomalies in 1983, 1989, and 1991 and with the 1983 season June-September 1983 being almost +1.2 times the standard deviation.

In the Sahel region of Africa (Fig. 5.8j) the model reproduces quite well the interannual variability of rainfall for the period, as depicted by the CMAP data, but there is systematic overestimation of the observed rainfall of more than 2 mm day$^{-1}$(Table 5.3). For this region, there are a number of studies linking rainfall variability to global SST anomalies. Currently, this is the baseline of the Hadley Centre prediction (Rowel et al., 1995). The skill of the CPTEC/COLA AGCM in simulating the year-to-year variability of precipitation in the Sahel is rather modest. However, the model captures well the interannual variability during the peak rainy season, with positive rainfall anomalies during 1985 and 1988/89, as well as the negative rainfall anomalies during 1983 and 1987.

Northwest Peru-Ecuador (Fig. 5.8 k) shows the abundant observed and modeled rainfall during the December 1982-February 1983 and December 1985-February 1986 periods, typical of El Niño years. In other regions of the world (not shown), a visual inspection of the observed and modeled rainfall indices does not reveal whether the model in fact yields a good representation of the interannual variability. In fact, the model overestimates rainfall in Southern Africa by more than 70%, and over eastern Africa by approximately 30%. As in the Amazon basin, the model underestimates rainfall in the Indonesian region between 40-50%. For regions such as Australia, Northern Argentina, and central Europe and along the SPCZ, the model reproduces the mean and standard deviations of rainfall amount during the 1982-91 period, although the interannual variability may not be well depicted. Feedbacks that go beyond the SST external forcing may be more important for some regions, and this seems to be the case of the Indian monsoon region as explained by Goswami (1998).

## 5.3 SKILL OF THE MODEL SIMULATIONS

As described in Section 4.4, the Brier skill score technique is used to assess rainfall anomaly simulations in several regions of the globe. To construct the Brier skill score, the grid point precipitation anomalies of the selected regions during the respective rainy seasons are averaged from each member to form the ensemble mean of the 9 values that are compared to the observed area averaged anomaly.

Table 5.3 shows small values of the BSS for northern and southern Northeast Brazil (0.13 and 0.07, respectively), Amazonia (0.33), and southern Brazil-Uruguay (0.47) indicate that the CPTEC/COLA AGCM is more capable of capturing interannual variations of MAM averaged rainfall in Northeast Brazil and Amazonia, and JJA averaged rainfall in Southern Brazil-Uruguay. For other regions such as India (0.97), Eastern Africa (0.51), Sahel (0.51), and Northwest Peru-Ecuador (0.67), the Brier scores are slightly greater than 0.5. Brier scores of 0.97 in Indian

monsoon and 0.67 in Northwest Peru indicating that the model is not as skillfull as other regions high higher predictability. Re-formulations in the physical parameterizations in some of the AMIP models (Sperber et al. 1999a) produce improvements in the Brier skill score for the Sahel, going from 0.64 to value of 0.5 after the re-formulations in the models, while for Northeast Brazil the scores were 0.13/0.08 before and after revisions in the models, and in the all Indian rainfall, the scores were 0.33/0.31 before and after the revisions.

**TABLE 5.3. BRIER SKILL SCORES FOR SOME REGIONS IN THE WORLD DURING THE PEAK OF THE RAINY SEASON, AS OBTAINED FROM THE CPTEC/COLA AGCM.**

| Region | Rainy season | Brier skill score |
|---|---|---|
| North-Northeast Brazil | MAM | 0.13 |
| South-Northeast Brazil | MAM | 0.07 |
| Southern Brazil-Uruguay | JJA | 0.47 |
| Amazonia | MAM | 0.33 |
| Northwest Peru-Ecuador | DJF | 0.67 |
| Indian monsoon | JJAS | 0.97 |
| Sahel | JJA | 0.51 |
| Eastern Africa | JJA | 0.51 |

Comparing the BSSs from Table 5.3 with those determined by Sperber et al. (1999a) for the AMIP simulations, their scores of 0.13 and 0.08 for the original and revised models, respectively, for Northeast Brazil as a whole, are very similar to the 0.13 and 0.07 values derived for both northern and southern Northeast Brazil during the MAM season of the CPTEC/COLA AGCM. The scores obtained by the CPTEC/COLA AGCM in regions such as India, Eastern Africa, the Sahel and Northwest Peru-Ecuador indicates that simulation of interannual variations of rainfall still remains problematic, possible due to land-surface feedback

mechanisms, and the need for better simulations of physical processes or SST in oceans other than the Pacific, such as the Indian Ocean.

Since Northeast Brazil rainfall distribution arises from different rainfall producing mechanisms across the region, we have subdivided the region in northern and southern sections. The score of southern Northeast for MAM is much lower (0.07) than that of northern Northeast for the same MAM season (0.13), indicating a better skill of the model in reproducing interannual variations of rainfall in southern Northeast Brazil as compared to northern Northeast Brazil. Also from Sperber et al. (1999a), their skill scores for their original and revised models are 0.33 and 0.31 for India, while our score estimated here is 0.97, and for Sahel the original and revised models produce scores of 0.64 and 0.58, while the CPTEC/COLA model derived score for the same season is 0.51.

The low BSS for Northeast Brazil (as a whole and the northern and southern sections) indicates a good skill of the CPTEC/COLA AGCM in simulating interannual rainfall variability during the peak of the rainy season in those regions. This is also corroborated by the reduced scatter among members of the ensemble (Figs. 5.8a, b) and the low spread among members, especially in Northeast Brazil. A relatively good model skill is also found along the Pacific ITCZ, Amazonia, and Northwest Peru-Ecuador (Figs. 5.8d, g, j).

A companion paper by Cavalcanti et al. (2001) estimates the Root Mean Square Errors (RMSE), correlation anomalies and the reproducibility of precipitation. In the Indonesia region the largest errors occur in DJF and JJA. Large errors also occur to the west of Central America in all seasons, and over south of Asia in JJA, which is consistent with the large BSS on those regions. The correlation is high over the tropical Pacific and Atlantic Oceans with very high values over eastern Pacific Ocean. Although there are errors related to intensity or position of the Atlantic and Pacific ITCZ, the anomalies are well represented. The correlation over Northeast Brazil is above 0.3 in all seasons. In MAM correlations of 0.5 extends to the whole

region. This is an important feature to rainfall prediction in this area that has the rainy season in MAM, which is also confirmed by the lowest BSS in Table 5.3. All of this indicates that the precipitation variability in these regions is well simulated by the model.

Reproducibility is another method of model validation, which measures the model's ability to respond consistently to the imposed boundary forcing (Sperber and Palmer, 1996). It can also measure the spread of the ensemble members, as in Stern and Miyakoda (1995) and has been calculated by Cavalcanti et al. (2001) for the general climatology of the CPTEC/COLA AGCM. The largest values of reproducibility are found in regions that show the lowest spread among members of the ensemble in Fig. 5.8: (a) the East Pacific in all seasons, consistent with Fig (5.8d), that shows the lowest spread among members along the Pacific ITCZ, and in agreement with Sperber and Palmer (1996) with ECMWF model results; (b) Northeast Brazil shows high values during MAM (Fig. 5.8a, b); (c) West Sahel in Africa (Fig. 5.8i) in JJA; (d) Norwest Peru and Ecuador (Fig. 5.8j) in DJF; (e) Amazonia (Fig. 5.8g) MAM. In this latter region, the reproducibility is lower (0.7-1.0) as compared to Northeast Brazil (1.0-2.0) or the Eastern Pacific-West Coast of Peru (1.0-4.0). Regions with large spread among members such as the monsoon region in South America (Fig. 5.8e) show reproducibility of 0.2-0.4, while in the monsoon area of North America and India (Fig. 5.8 f, h) the values reach values between 0.2-0.5 in the northern section of India. These regions with low reproducibility and large spread among members, also exhibit relatively larger RMSE. For more information on the reproducibility and the RMSE analyses, refer to Cavalcanti et al. (2001).

## 5.4 CASE STUDIES OF EXTREME EVENTS: THE 1982/83 EL NIÑO AND 1998/89 LA NIÑA

Based on the analysis presented in Sections 5.1-5.3, the following case study analysis focus on the 1982/83 El Niño and 1988/89 La Niña events. Even though

these two events may have been previously studied, they provide a great opportunity to test the sensitivity of the CPTEC/COLA AGM to SST changes, and to investigate if it captures the large-scale features of circulation, convection and rainfall associated with these extremes of ENSO. Our analysis in the previous sections indicates that the model seems to be more sensitive to warm El Niño SST forcing than to cool SST La Niña, as described in Sections 5.1 and 5.2 on more detail.

### 5.4.1 LARGE SCALE ANALYSIS: EAST-WEST EQUATORIAL CIRCULATION AND TROPICAL-MIDLATITUDE TELECONNECTIONS

Large-scale forcing associated with tropical Pacific SST influences the large-scale east west overturning in the atmosphere and thus the east-west mean zonal circulation (Walker circulation in the Pacific), as well as the monsoon and other circulation regimes around the world. Interannual rainfall variability in tropical South America is closely linked to changes in intensity and position of the SST in the tropical Pacific and Atlantic. Extreme phases of SO have a significant impact on the overall strength of the Walker circulation and in rainfall in the west coast of South America, as well as the east-west circulation in the tropical Atlantic and adjacent Amazonia and Northeast Brazil. Figs. 5.9a-h show vertical wind field anomalies during DJF and MAM 1982/83 and 1988/89, as derived from the CPTEC/COLA AGCM and from the NCEP reanalyses for a band between 5 °N-5 °S. DJF is the peak of the rainy season in Northwest Peru and MAM is the peak of the rainy season en central Amazonia, the mouth of the Amazon region and North Northeast Brazil.

As the central equatorial Pacific is anomalously warmer than average during the 1982/83 El Niño (Fig. 5.9a-d), upward vertical motion over tropical South America west of the Andes and the adjacent eastern Pacific is enhanced, as depicted by the NCEP reanalyses during DJF (Fig. 5.9a) and MAM (Fig. 5.9c). These circulation features are well captured by the model for both seasons (Fig. 5.9b, d).

Over tropical South America east of the Andes, both model and the reanalyses exhibit subsidence anomalies, while on the eastern and central Pacific, the model reproduces the observed stronger than normal upward vertical motion. Compensatory subsidence to the east of the Andes is also observed over central Amazonia and Northeast Brazil, which is also consistent with the anomalously northward displaced ITCZ over the Atlantic sector and reduced northwest trades and moisture transport into Amazonia during the MAM 1983 (Marengo and Hastenrath 1993), and this situation is well reproduced by the CPTEC/COLA AGCM.

During the 1988/89 La Niña event (Fig. 5.9e-h), when central equatorial Pacific SSTs are cooler than normal, rising motion is weaker than normal in this section of the Pacific and the adjacent Peru-Ecuador coast, and subsidence anomalies are shown in both model and observations for both DJF (Fig. 5.9e-f) and MAM (Fig. 5.9g-h). The anomalously strong observed rising motion over eastern Amazonia and northern Northeast Brazil, during DJF and MAM peak of the rainy season of the above regions is well reproduced by the model.

An example of the dynamical response to variations in tropical Pacific SST in the upper levels is the PNA pattern in the Pacific North American sector. Early work by Wallace and Gutzler (1981); Blackmon et al. (1984); and Pandolfo (1993) explain that the position of the centers of action of the PNA, are successively the equatorial central Pacific, north central Pacific, western Canada and southeastern United State, apparently along a great circle route. During the El Niño 1982/83 and the El Niño 1997/98 (Barsnton et al., 1999), the enhanced easterly flow in the upper troposphere produced an anomalous anticyclonic couplet at both hemispheres over the tropical central Pacific, which is shown in Fig. 5.10a from the 200 hPa 1982/83-1988/89 differences, and in less degree in Fig. 5.10b from the model difference, showing instead a region of negative height anomalies between 15 °N-15 °S over the tropical Pacific and two centers of positive height anomalies over Southeast Asia and New Zealand, not seen in the observations.

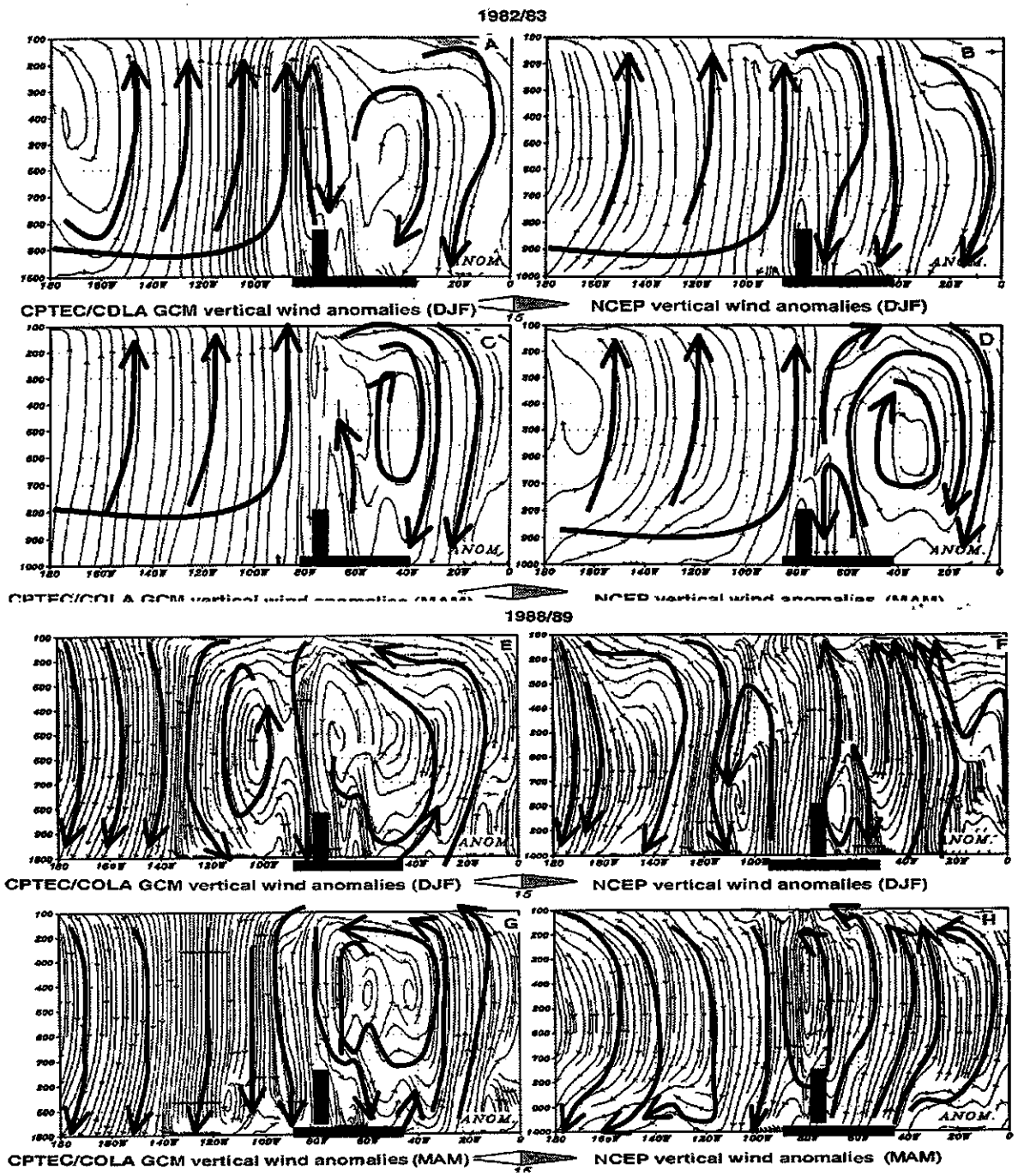


Fig. 5.9 - Pressure-longitude section of anomalous vertical velocity circulation (5 $^{O}$N-5 $^{O}$S) for DJF 1982/83 (a, b), MAM 1988/89, (c, d), DJF 1988/89 (e, f) and MAM 1988/89 (g, h). Shading contours represent speeds higher than 15 ms$^{-1}$. Anomalies are departures from the 1982-91 base period. South America is represented by the black boxes.

At higher latitudes, the model response resembles the structure of the observed PNA, with a positive 200 hPa height anomaly over central and eastern Canada, that appears comparable to Bamston's analysis for 1983, 1987 and 1998 El Niños, and the model reproduced this center in terms of intensity and position (Fig. 5.10a, b). Anomalous large negative height anomalies (and cyclonic circulation anomalies) over the Gulf of Alaska and the Aleutian Island are well depicted by the model, and are also a typical pattern of other very strong El Niños. The observed negative 200 hPa height anomaly map (Fig. 5.10b) in the North Pacific shows large intense negative height anomalies, that is comparable in sign but not in intensity with the model derived height difference (Fig. 5.10a). This could be related to the tendency of the CPTEC COLA AGCM to underestimate sea level pressure on the North Pacific (Cavalcanti et al. 2001). Differences between the greater intensity of height anomaly south of the Aleutians in 1982/83 as compared to 1997/98 (CPTEC, 1998) could be a consequence of a more westerly location of the strongest SST anomalies in early 1983. Over Southeast United States, a center of negative observed height anomalies is well depicted by the model, although it is somewhat weaker and displaced slightly to the north.

### 5.4.2 MONSOON SYSTEMS IN THE INDIAN AND SOUTH AMERICAN SECTORS

The monsoon is a coupled ocean-land-atmosphere phenomenon, and it varies by imposition of a remote forcing or by its own variability inherent in the coupled ocean-atmosphere systems in some combination. Magaña and Webster (1998) presented a comprehensive review on the monsoon systems and their variability and prediction in the Indian-Southeast Asia and in Central-North American sector, while a study by Zhou and Lau (1998) have documented the presence of a monsoon system in South America. From the analysis of Fig. 5.8e, f, h, it was observed the large spread among members of the ensemble while trying to predict rainfall anomalies at the peak of the rainy season, and perhaps the worse

predictability (large scatter among members) occurs in the South American monsoon region (Fig. 5.8e).

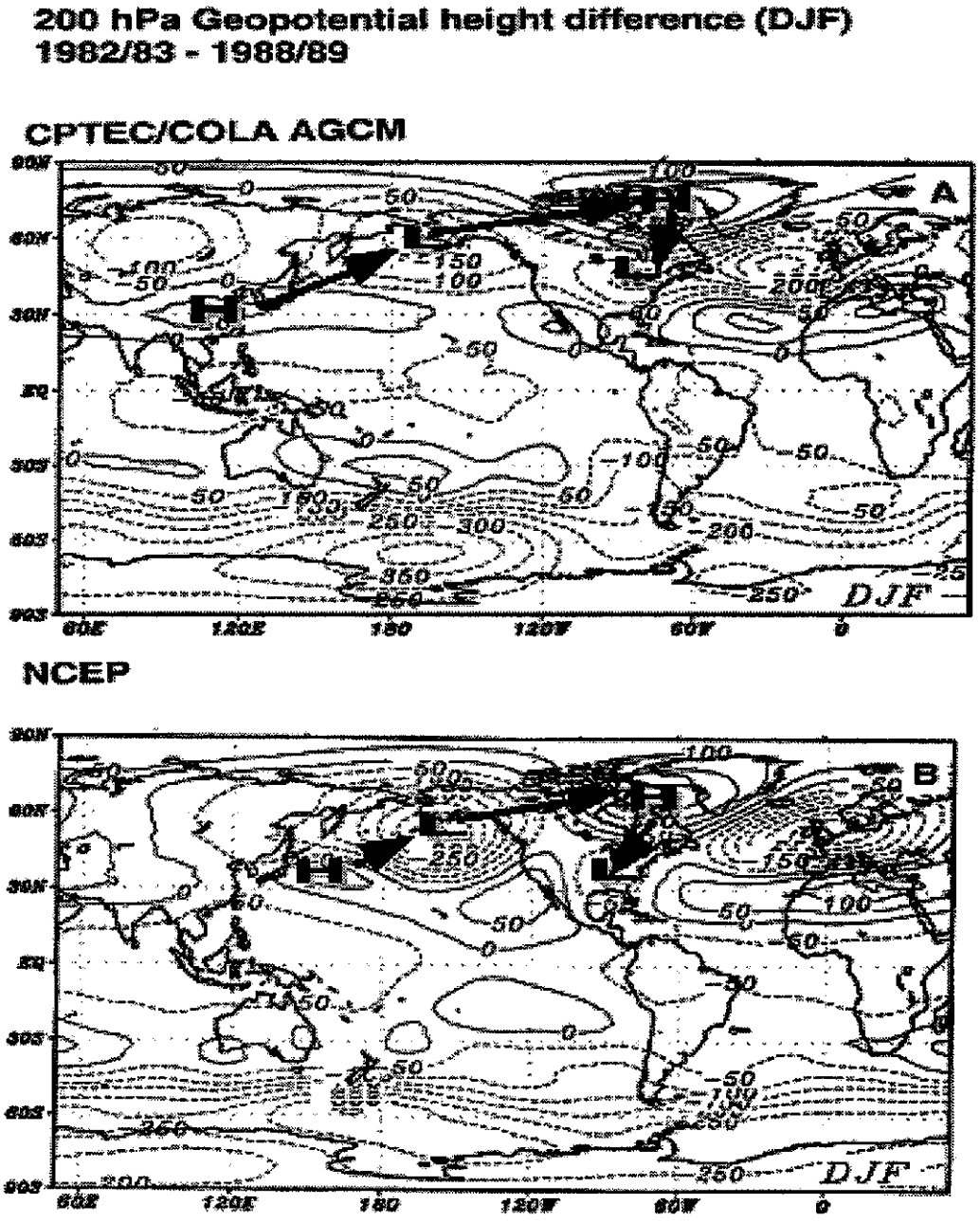


Fig. 5.10 - The 200 hPa height difference fields for DJF 1982/83 minus DJF 1988/89, as (a) produced by the ensemble mean of the of the CPTEC/COLA AGC, and (b) from the NCEP/NCAR reanalysis.

Several theories than try to explain the interannual variability of the Indian monsoon, and that may or may not applied to the American monsoon systems are based on: (a) the monsoon is a "slave" to the external forcing of the ENSO cycle, even though the SOI accounts for about 35% of Indian monsoon rainfall variability (Magaña and Webster, 1998); (b) the monsoon can be strong or weak depending on the state of snow or ground moisture on the Eurasian continent during spring, which can also may be applicable for South America; and (c) the impact of ENSO on the monsoon in Asia and South America is a function of phase.

As indicated in Section 5.1, a large spread in simulation of the rainy season in the Indian and South American monsoon regions occurs among ensemble members of the same model, or between integrations by different models (Sperber et al. 1999a; Webster et al., 1998), and is also depicted in Fig. 5.8h for Indian monsoon, while the predictability in South America is low. The degree of predictability depend on slowly varying boundary conditions, as SST, but the monsoon system is chaotic and there are inherent limitations to prediction. Thus, the question is whether or not the spread of simulations of Indian and South American monsoon is because model inadequacies or because of chaotic elements in the monsoon region.

The following discussion is based on comparisons between observed and modeled circulation and rainfall features of the Indian and South American monsoon systems from section 5.1, but with more emphasis on extreme situations linked to 1982/83 El Niño and the 1988/89 La Niña events. In here, besides the fact that we want to assess the ability of the CPTEC COLA AGCM in depicting the circulation and rainfall anomalies associated with these two extreme events, as well as the sensitivity of climate in those regions to an external forcing, as it was with the SSTs anomalies in the equatorial Pacific.

For the Indian summer monsoon, Fig. 15.11a-h shows the observed (panels a, c, e, g) and modeled (panels b, d, f, h) for the JJA 850 hPa flow and CMAP rainfall during 1983 and 1989 events. In both cases the model reproduces the major

monsoon features, mainly the strong Somali low-level jet, the southerly flow inland into the Asian continent from the Arabian Sea and from the Bay of Bengal and across the Southeast Asia towards the northwest Pacific. However, major differences appear in both years over the western Pacific-southeast Asian region, where the model does not reproduce the easterly flow over the western Pacific. In both years the model underestimates the precipitation over west tropical Pacific. Furthermore, modeled rainfall in 1983 reproduces the observed rainfall over the west coast of India and the Bay of Bengal (Fig. 5.11a, b), while in 1989 the model produces less rainfall than the observed over India and also produces excessive rainfall over Sumatra.

The model shows negative rainfall anomalies during JJA 1983 (Fig. 5.11f) over northern and western India, associated with weaker southerly flow over India and an anticyclonic anomaly over northern India. These features contrast with the observed negative rainfall anomalies over western India, and the relatively strong southerly flow and a cyclonic circulation anomaly depicted by the NCEP reanalyses over eastern India. Fig. 5.11f also exhibits intense anticyclonic anomalies further to the south over the Indian Ocean (15 °S) that is captured by the model with less intensity. For 1989, the observed fields (Fig. 5.11d) shows an anticyclonic anomaly over the Arabian sea around 5 °N, possibly reducing westward moisture transport, and thus convection and rainfall over the region. The model shows a deficiency of rainfall over 5 °N and 140 °E during JJA 1983 (Fig. 5.11e) related to the eastward wind anomalies over the western equatorial Pacific, which contrasts with the observed strong westward anomalies o negative rainfall anomalies cover most of the western tropical Atlantic. The model does not reproduce the strong easterly wind anomalies along the equator during JJA 1989 (Fig. 5.11g, h).

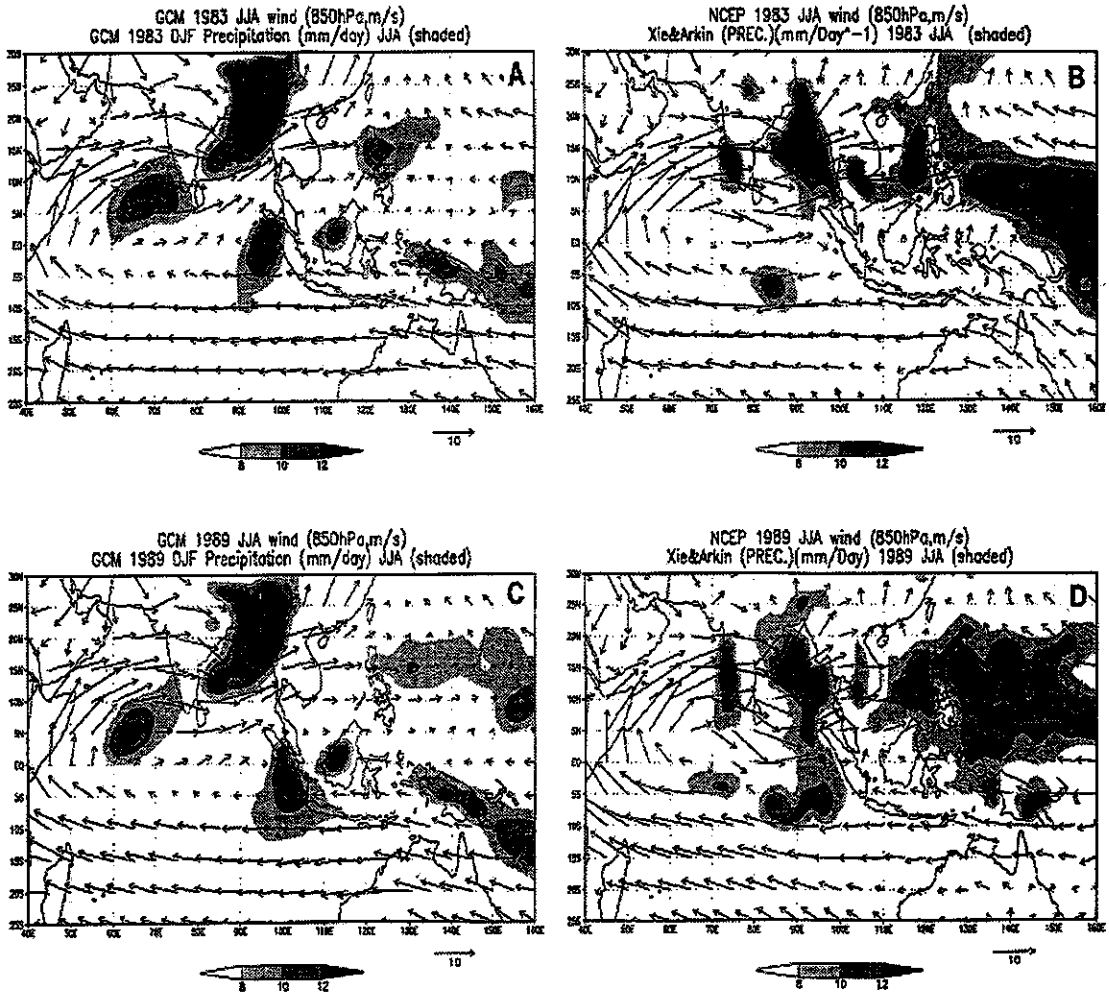


Fig. 5.11 - Low level circulation (850 h-Pa) and rainfall for the Indian-Southern Asian monsoon area. Scale for the winds is shown at the lower right side of each panel and the gray scale of rainfall is shown on the lower side of each panel. Panels a-d represent the JJA 1983 and panels e-h represent JJA 1989. Model circulation and rainfall are presented in the right panels (b, d, f, h) and NCEP/NCAR reanalyses are indicated on the represent the left side panels (a, c, e, g). Panels a, b, e, f show the actual fields, and panels c, d, g, h show anomalies from the base period 1982-91. (continua)

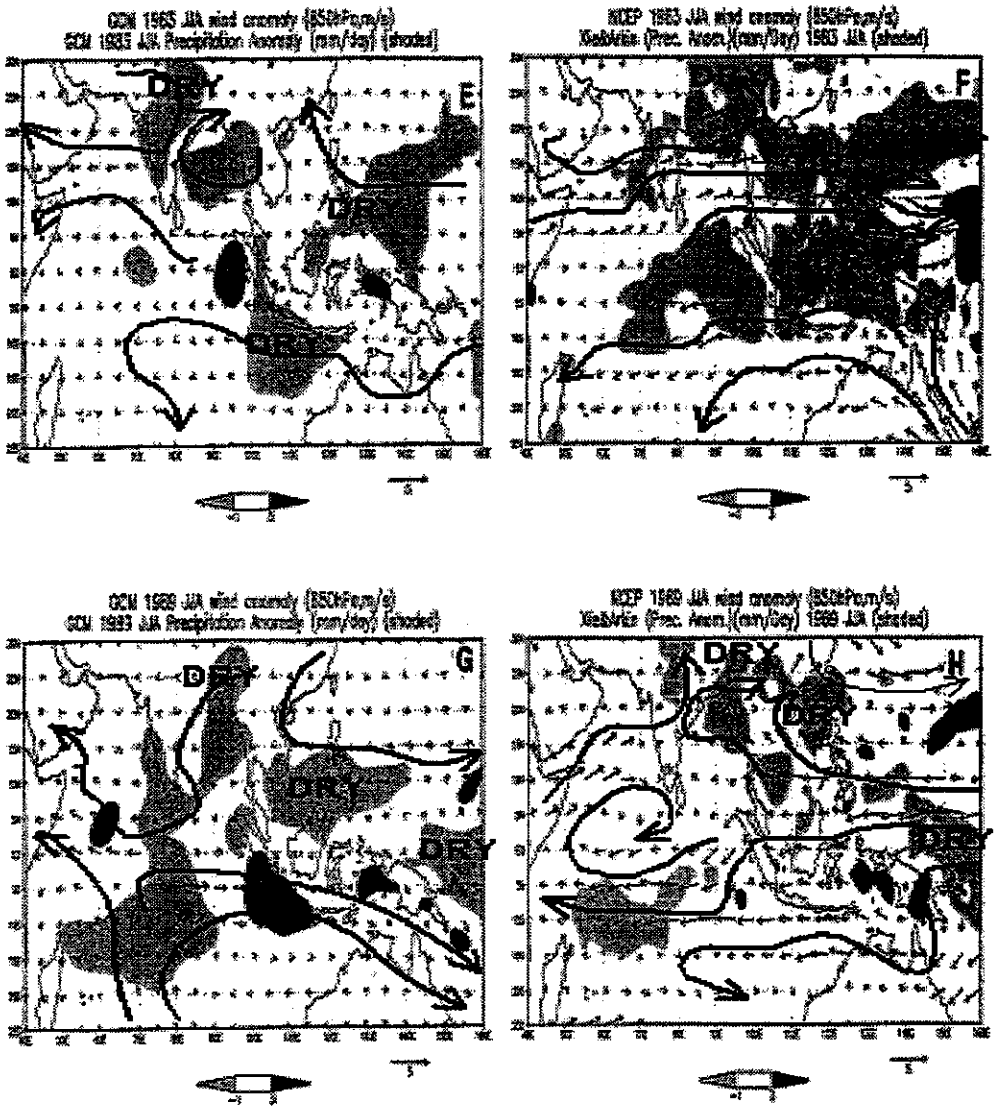


Fig. 5.11 (conclusão)

In relation to the South American monsoon, Figs. 5.12a-h should be analyzed in conjunction with Fig. 5.5a and 5.8e. The model reproduces the major

climatological features of the monsoon of South America, in relation to the surface circulation, the upper-tropospheric Bolivian anticyclone, rainfall over the region, and the low-level jet east of the Andes. For DJF 1982/83 (Fig. 5.12a, b, e, f), the model depicts the near surface circulation east of the Andes quite well, and the convergence and rainfall fields show a very intense SACZ and anomalously southward displaced SACZ between 15 and 30 °S, while the northeast section of it, that appears in the CMAP rainfall fields, is not reproduced by the model in both 1982/83 and 1988/89. The SACZ is stronger and wider during 1988/89 as compared to 1982/83. As shown in Fig. 5.5 b, the mode also shows some systematic errors in the depiction of the Bolivia high, and also de Northeast Brazil upper level trough.

### 5.4.3 CIRCULATION, CPNVECTION AND RAINFALL OVER THE AMAZON RAINFALL OVER THE AMAZON BASIN

The near surface wind fields between 5 °N and 5 °S from eastern Amazonia towards the tropical Atlantic calculated by the model are weaker and too zonal as compared to observations. Te model also produces an anticyclonic anomaly centered at 20 °S, nearby the SACZ and the monsoon region, and negative rainfall anomalies along the SACZ, during DJF 1982/3, which is replaced by a cyclonic anomaly during 1988/89. A systematic error of the CPTEC/COLA AGCM is a rain shadow from 10 to 25 °S to the east of the Andes, and a "dry corridor" between central and eastern Amazonia. In both events, the model shows a realistic Atlantic ITCZ, especially during 1988/89, while the continental part of the SACZ is weak or absent.

Furthermore, the trade winds east of the Andes along equatorial latitudes tend to be too zonal and south of 10 °S they tend to converge depicting an anomalously strong convection and a more robust SACZ, stronger in DJF 1988/89 as compared to 1982/83, but present in both cases.

As discussed from Fig. 5.8 and in Section 5.1, the CPTEC/COLA AGCM underestimates rainfall systematically over northern and central Amazonia, although the model reproduces quite well the interannual variability, with a decrease (increase) of rainfall during strong El Niño (La Niña). The model shows a tendency for a southwestward displacement of the upper-level Bolivian High. This could be associated with the reduced modeled rainfall over north-central Amazon, and over the northeast portion of the SACZ, as well as the South American monsoon region.

The connection between the South American monsoon and the Amazon basin heat source (and consequently the Hadley circulation in the Atlantic sector) is clear, and systematic bias in one will affect the other. Reasons for these biases are to be discussed in the following section, in terms of the processes involving topography, parameterizations of components of the physical climate and their interactions (e.g. convection and clouds processes, land surface interactions, SST and ice feedbacks, etc).

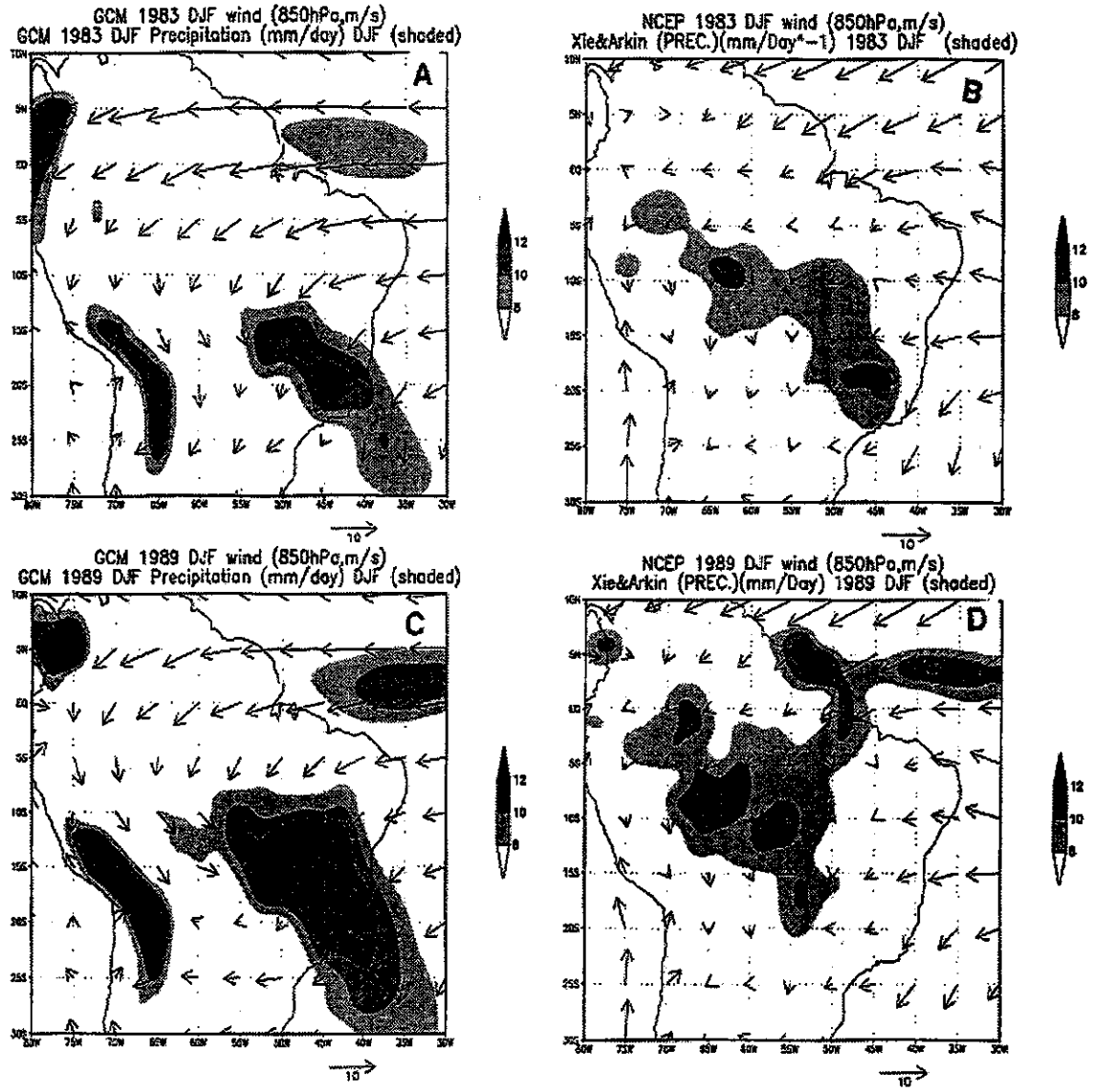


Fig. 5.12 - Low-level circulation (850 h-Pa) and rainfall for tropical South America. Scale for the winds is shown at the lower right side of each panel and the gray scale of rainfall is shown on the lower side of each panel. Panels' a-d represent the DJF 1982/83 and panels' e-h represent DJF 1988/89. Model circulation and rainfall are presented in the right panels (b, d, f, h) and NCEP/NCAR reanalyses are indicated on the represent the left side panels (a, c, e, g). Panels a, b, e, f show the actual fields, and panels c, d, g, h show anomalies from the base period 1982-91 (continua)

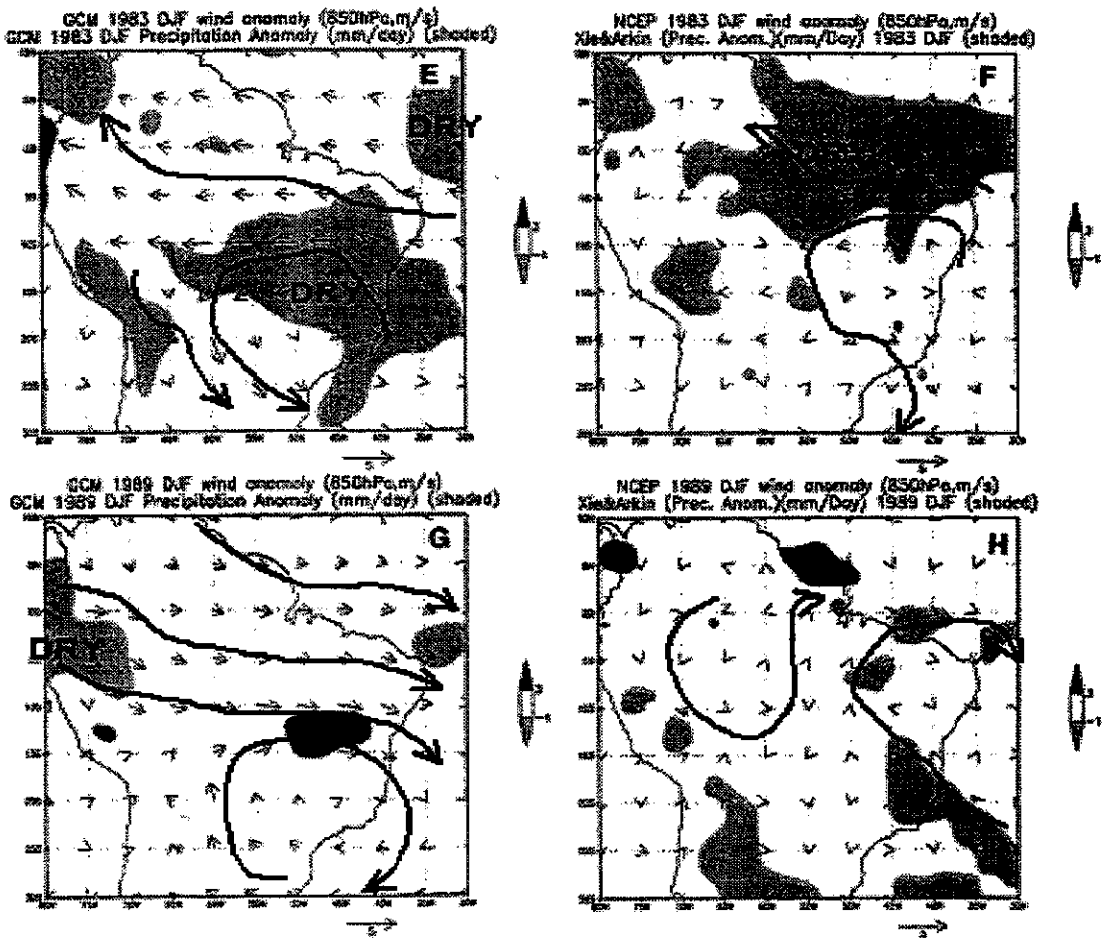


Fig. 5.12 - (conclusão)

# CHAPTER 6

## DISCUSSIONS

The CPTEC/COLA AGCM provides a realistic portrayal of the interannual variability of rainfall and large-scale circulation. The model responds very well to a large scale SST forcing in the tropical oceans, and hence can reproduce many facets of interannual climate variability in several regions in the tropics, mid and high latitudes. Improvement of the simulation of interannual variability is associated with a better simulation of the observed climatology by the models, and this holds true for the CPTEC/COLA AGCM. As in several other climate models, model simulations with climatological SSTs could capture the most prevalent anomaly patterns observed in the atmosphere, and seems to be especially true for large SST anomalies, such as those typical of ENSO in the central equatorial Pacific.

However, some aspects of ENSO are still not well captured by our model, nor by any other present-day atmospheric or coupled models. Latif et al. (1999) analyzed the SST climatology and interannual variability simulated by 24 models in the Equatorial Pacific, and found that when compared with observations, about half of the models are characterized by too weak interannual variability in the eastern equatorial Pacific, while models generally have larger variability in the central equatorial Pacific. They also found that the majority of the models show a weak Indian monsoon associated with the model ENSO. This latter is also true for the CPTEC/COLA AGCM. It is possible that phenomena of climate variability, such as El Niño, are sensitive to orographic effects and their parameterization in the different models, including the CPTEC/COLA AGCM.

The mean position and seasonal migrations of major rain belts in South America, Africa and Indonesia-Southeast Asia are well simulated, however some "dry" spots have been found in Amazonia, western Pacific and equatorial humid Africa in the

summer hemisphere. Coarse resolution climate models may fail to give satisfactory simulations in Southeast Asia, East Africa and North American monsoons, and an increase in horizontal resolution can improve precipitation details, but is not sufficient to remove large-scale model biases. The T62 horizontal resolution (considered as fairly high) of the CPTEC/COLA AGCM still shows problems in tropical rainfall and major tropical-subtropical convergence zones. These shortcomings can also be related to the physical parameterizations and small changes in them can make a significant difference in the amplitude of the simulated SST forcing tropical rainfall and mid-latitude height anomalies. Especially, problems in the land surface parameterizations can produce important feedbacks on the monsoon circulation and rainfall (Ferranti et al., 1999).

Recent atmospheric models with revised physical parameterizations show improved interannual variability of the all-India rainfall, Indian/Asian monsoon wind shear, Sahel and Northeast rainfall (Sperber et al., 1999a). For instance, the revised BMRC AGCM shown in Sperber et al. (1999a) contains the Tiedtke scheme replacing the Kuo convection, and exhibits much better interannual variability of rainfall for Northeast Brazil, as compared to the older version of the AGCM. To improve our confidence in the simulation of land surface processes that may affect interannual variability of the Indian Monsoon, such as snow and soil moisture and their feedbacks, significant advances are required in the simulation of snow, liquid and frozen soil moisture and their associated water and energy fluxes, in regions such as the Himalayas.

The CPTEC COLA AGCM uses the Kuo deep convection, scheme, and by replacing it with the relaxed-Arakawa Schubert, or RAS scheme (Pezzi and Cavalcanti, 2000) both schemes have some problems depicting the SACZ and rainfall in Amazonia, on in the Northern hemisphere the errors in rainfall and circulation are lesser with the RAS scheme than with the Kuo scheme.

For the Amazon basin, the GISS AGCM exhibited the same problem as the CPTEC/COLA AGCM, with systematic underestimation of rainfall in the region, possibly due to unrealistically high evaporation, affecting not only the thermal and energy regime near the surface, but also the runoff, which was also largely underestimated. The new land-surface and ground hydrology scheme in the GISS AGCM (Marengo and Druyan, 1994; Marengo et al. 1994) produces more realistic evaporation, and a slight increase in boreal summer-fall precipitation in the basin.

The low spread within the ensemble for rainfall simulations in Northeast Brazil, Amazonia, and the ITCZ region in the Atlantic, as well as the Sahel, Northwest Peru few other regions indicates that the skill of the model is good for those regions. The lower Brier Skill scores derived for those regions confirm this. There are few exceptions, such as the monsoon regions of the world where the spread is large, thus implying that other forcing than the external SST may be important on climate variability on those regions.

# CHAPTER 7

## SUMMARY AND CONCLUSIONS

This study summarizes the interannual climate variability of a 9-member ensemble, 10-year simulation of the CPTEC/COLA AGCM for the period 1982-1991, forced with observed SST. A companion study (Cavalcanti et al., 2001) describes the surface and upper-air climatological aspects simulated by the model and its validations against observations. In general, the CPTEC/COLA AGCM model is relatively successful in depicting rainfall and circulation features in the tropics in the presence of large SST anomalies. This enhanced predictability is not unique to our model, since several other models have produced similar simulations, as the AMIP Project can show. However, in the absence of significant SST anomalies, there is a large spread among members of the ensemble, especially in regions of low predictability, such as the monsoon areas of India and the Americas.

In general, the model represents reasonably well the observed circulation and rainfall, as well as their interannual variability at different latitudinal bands, even though there is a tendency for the model to systematically overestimate the actual amount of rainfall, in both mid and high latitudes, and in a lesser degree in the tropics. The model also shows a reasonable simulation of the interannual variability of climate in the tropical-equatorial region, especially the zonal migration of the convective and rainfall bands during the 1982/83 and 1986/87 El Niño events over the western and central equatorial Pacific, and over the Amazon-Northeast Brazil regions east of the Andes.

Rainfall variability in extreme years, due to migrations of the ITCZ in the tropical Atlantic and Pacific regions, are well reproduced, both in magnitude and variability, indicating an enhanced model skill in the tropics and equatorial regions associated with ENSO-related SST forcing. The South Pacific Convergence Zone (SPCZ) is well represented, especially its behavior during the strong El Niño 1982/83 and La

Niña 1988/89, however there is a relatively large scatter among members of the ensemble, indicating problems with the model low-level convergence and convection over that region.

The model rainfall and circulation present some problems over the Amazon and South American monsoon regions. There is a systematic error in the location of the year-to-year position of the upper-tropospheric Bolivian High, which may be responsible for the systematic underestimation of summertime convection and rainfall in Amazonia. While the model shows less convection and rain in central and northern Amazonia in summertime, more convection and rainfall is shown over the Panana-Colombia coast and the SACZ.

In India-Southeast Asian sector, the model captures well the variability of the upper-tropospheric Tibetan High, and on the surface circulation it depicts well the Somali Jet, and the inland southerly flow over the Arabian Sea and the Bay of Bengal. However it fails to generate the correct surface circulation over the extreme western Pacific region, inhibiting moisture convergence and convection and producing less rainfall than observed over the Western Pacific. Other factors besides the external forcing (SST anomalies) more related to the internal climate variability, besides SSTs, may be responsible for a substantial part of the interannual climate variability of these regions.

Interannual variability of rainfall in Northeast Brazil (northern and southern sections), Amazonia, and southern Brazil-Uruguay and in Northwest Peru-Ecuador is well simulated by the CPTEC/COLA AGCM, while more modest success is found over India and Eastern Africa and the Sahel, owing in part to the strong links to Tropical Atlantic and Pacific SSTs. Better model predictability and high skills are found in Northeast Brazil, Amazonia, while Sahel shows a relatively good skill, lower skills are found over regions such as the monsoon regions.

The strengths and weaknesses identified in this model should not be regarded as permanent defects, since the model is undergoing continuous improvement. It is clear that some areas exhibit systematic biases, such as the underestimation of rainfall in Amazonia and an overestimation of rainfall in the Sahel. On the whole, the CPTEC/COLA AGCM simulates the broad aspects of the observed ENSO variations reasonably well, as may be expected since prescribed SST primarily drives these variations.

In general, the simulated interannual variability of the model compares well to observations. Over the tropics the model simulates a clear eastward-propagating anomaly in tropical convection and rainfall during events of anomalously warm tropical Pacific associated with El Niño events. This signal is evident in the zonal winds and convection too.

For several regions of the planet, other factors beyond the external forcing provided by SST anomalies may be important in their year-to-year climate variability, suggesting limitations on climate predictability over those regions, and our analyses show relatively lower skill of the CPTEC/COLA AGCM, as in the Indian monsoon area. As indicated by Shukla et al. (2000a), the prospects for climate simulation and prediction should not be considered hopeless even for years when SST anomalies are not large, because model still have quite large systematic errors which need to be reduced. The possible influence of land surface boundary conditions (snow, soil moisture) in improving seasonal predictability also needs to be investigated.

Further investigation is needed to explore the question of weather increasing the ensemble size, either by making a larger number of integrations with the same model or by combining integrations of several models would lead to a better climate predictions, either the mean climate and its seasonal to interannual variability.

This study along with its companion paper dealing with the simulated mean state, aims at assessing the ability of the CPTEC/COLA AGCM to simulate the observed climate and its interannual variability.

**Acknowledgements**

J.A. Marengo, I. Trosnikov and C. D'Almeida were partially supported by the Brazilian Conselho Nacional de Desenvolvimiento Cientifico e Tecnologico (CNPq). We thank NCAR for providing access to the NCEP/NCAR reanalyses, and to Ping Ping Xie for providing the CMAP rainfall data sets.

## REFERENCES


Barnett, T. Monte Carlo climate forecasting. **Journal of Climate**, v.8, p. 1005-1022. 1995.

Bamston, A.; Leetma, A.; Kousky, V. E.; Livezey, R. E.; O'Lenic E.A.; Van den Dool, H.; Wagner, J.; Unger, D. A. NCEP forecasts of the El Niño of 1997-98 and its U.S. impacts. **Bulletin American Meteorological Society**, v.80, p. 1829-1853. 1999.

Bengtsson, L.; Arpe, K.; Roeckner, E.; Schulzweida, U. Climate predictability experiments with a general circulation model. **Climate Dynamics**, v.12, p. 261-278. 1996.

Blackmon, M., L.; Lee, Y. H.; Wallace, J. M. Horizontal structure of 500 mb height fluctuations with long, intermediate and short time scales. **Journal Atmospheric Sciences,** v. 41, p. 961-979. 1984.

Bonatti, J. P. Modelo de Circulação Geral Atmosferico do CPTEC. **Climanalise Especial**. v .11, p. 198-202. Outubro 1996. Available from CPTEC/INPE, Rodovia Dutra km. 40, 12630-000 Cachoeira Paulista, SP, Brazil.

Brankovic, C.; Palmer, T. Atmospheric seasonal predictability and estimates of ensemble size. **Monthly Weather Review**, v. 125, p. 859-874, 1997.

Brankovic, C.; Palmer, T.; Ferranti, L. Predictability of seasonal atmospheric variations. **Journal of Climate**, v. 7, p. 217-237. 1994.

Cavalcanti, I. F.A.; Nobre, P.; Trosnikov, I. Simulação de verão e outono de 92/93 e 93/94 com o GCM CPTEC/COLA. In: Congresso Brasileiro de Meteorologia N° 9, Campos do Jordã, **Anais.** p. 807-811, 1996.

Cavalcanti, I. F. A.; Pezzi, L. P.; Nobre, P.; Sampaio, G.; Camargo, H. Climate prediction of precipitation in Brasil for the Northeast raining season (MAM) 1998. **Experimental Long -Lead Forecast Bulletin,** v. 7, p.24-27. 1998.

Cavalcanti, I. F. A.; Pezzi, L. P.; Sampaio, G.; Sanches, M. B. Climate prediction of precipitation in Brasil for the Northeast raining season (MAM) 1999. **Experimental Long -Lead Forecast Bulletin,** v. 8, p. 25-28. 1999.

Cavalcanti I. F. A.; Satyamurty, P.; Marengo, J. A.; Trosnikov, I.; Bonatti, J.P.; Nobre, C. A,; D'Almeida, C.; Sampaio, G., Cunningham, C. A. C.; Camargo, H.; Sanches, M. B.; Climatological features represented by the CPTEC/COLA Global Climate Model. **Climate Dynamics**, 2001. Submitted.

Davies, J.; Rowell, D.; Folland, C. North Atlantic and European seasonal predictability using an ensemble of multidecadal atmospheric GCM simulations. **International Journal of Climatology**, v. 17, p.1263-1284, 1997.

Ferranti, L.; Slingo, J. M.; Palmer, T. N.; Hoskins, B. J.; The effects of land surface feedbacks on the monsoon circulation. **Quarterly Journal Royal Meteorological Society**, v. 125, p. 1527-1550. 1999.

Figueroa, S. N.; Satyamurty, P.; Silva Dias, P. L. Simulations of the summer circulation over the South American region with an Eta coordinate model. **Journal of Atmospheric Sciences**, v. 52, p. 1573-1584. 1995.

Garreaud, R.; Wallace, M. J. Summertime incursions of mid-latitude air into subtropical and tropical South America. **Monthly Weather Review,** v. 126, p. 2713-2733. 1998.

Garreaud, R. A multi-scale analysis of the summertime precipitation over the Central Andes. **Monthly Weather Review,** v. 127, p. 901-921. 1999.

Gates, W. L. AMIP, the Atmospheric Model Intercomparison Project. **Bulletin American Meteorological Society,** v. 73, p.1962-1970, 1992.

Gates, W. L.; Boyle, J.S.; Covey, C.; Dease, C. G.; Doutriaux, C. M.; Drach, R. S.; Florino, M.; Gleckler, P.; Hnilo, J.J.; Marlais, S. M.; Phillips, T. J.; Potter, G. L.; Santer, B. D.; Sperber, K. S.; Taylor, K. E.; Williams, D. N. An Overview of the results of the Atmospheric Model Intercomparison Project (AMIP I). **Bulletin American Meteorological Society,** v. 80, p. 29-56. 1999.

Goddard, L.; Mason, S. J.; Zebiak, S.E.; Ropelewski, C. F.; Basher, R.; Cane, M, A. Current approaches to seasonal to interannual climate predictions. **International Journal of Climatology**. 2001. In Press.

Goddard, L.; Graham, N. The importance of the Indian Ocean for simulating rainfall anomalies over eastern and Southern Africa. **Journal Geophysical Research.**, v. 104, p. 19099-19116. 1999.

Goswami, B.N.; Krishnamurty, V.; Saji, N H. Simulation of ENSO related surface winds in the tropical Pacific by an atmospheric general circulation model forced by observed sea surface temperature. **Monthly Weather Review**, v. 123, p. 1677-1694. 1995.

Goswami, B. N. Interannual variations of Indian Summer Monsoon in a GCM: external conditions versus internal feedbacks. **Journal of Climate**, v. 11, p.501-522. 1998.

Harzallah, A.; Sadourny, R.; Internal versus SST-forced atmospheric variability as simulated by an atmospheric general circulation model. **Journal of Climate**, v. 8, p. 474-495. 1995.

Hastenrath, S. **Climate of the Tropics.** Dordrecht, Boston, London, Kluwer Academic Publishers, 1996.

Instituto Nacional de Pesquisas Espaciais-Centro de Previsão de Tempo e Estudos Climaticos (INPE-CPTEC). **Projeto El Niño 1997-98**. Available from http://www3.cptec.inpe.br/pesquisas/clima/proelni97/indexelni.html, 1998

Janowiak, J. E.; Krueger, A.; Arkin, P.; Gruber, A. **Atlas of Outgoing Longwave Radiation derived from NOAA Satellite Data**, Greenbelt, MD, USA. NOAA Atlas N° 6, 1985. 44 p.

Kalnay, E.; Kanamitsu, M.; Kistler, R.; Collins, W.; Deaven, D.; Gandin, L.; Iredell, M.; Saha, S.; White, G.; Woollen, J.; Zhu, J.; Chelliah, M.; Ebisuzaki, W.; Higgins, W.; Janowiak, J.; Mo, K.; Ropelewski, C.; Wang, J.; Leetmaa, A.; Reynolds, R.; Jenne, R.; Joseph, D. 1996: The NCEP/NCAR 40-year reanalysis project. **Bulletin American Meteorological Society**, v. 77, p. 437-471. 1996.

Kawamura, R.; Sugi, M.; Sato, N. Interdecadal and interannual variations over the North Pacific simulated by a set of three climate experiments. **Journal of Climate,** v. 10, p. 2115-2121. 1997.

Kiehl, T. J.; Hack, J. J.; Bonan, G.; Boville, B. A.; Williamson, D.; Rasch, P. The National Center for Atmospheric Research Community Climate Model CCM3. **Journal of Climate.** v. 11, p. 1131-1150. 1998.

Kinter III, J. L.; De Witt, D. G.; Dirmeyer, P. A.; Fennessy, M. J.; Kirtman, B. P.; Marx, L.; Schneider, E. K.; Shukla, J.; Straus, D. M. **The COLA atmosphere-**

**biosphere general circulation model.** Calverton, MD, USA. 1997. COLA Tech. Report N° 51. 45 p.

Kitoh, A. Interannual variation in at atmospheric GCM forced by the 1970-89 SST. **Journal of the Meteorological Society Japan**, v.69, p.251-269. 1991.

Kumar, A.; Hoerling, M. Interpretation and implications of the observed inter-El Niño variability, **Journal of Climate,** v. 10, p. 83-91. 1997.

Kumar, A.; Hoerling, M. Annual cycle of Pacific/North American seasonal predictability associated with different phases of ENSO. **Journal of Climate**, v. 11, p. 3295-3308. 1998.

Latif, M.; Biercamp, J.; von Storch, H.; McPhaden, M. J.; Kirk, E. Simulation of ENSO related surface wind anomalies with an atmospheric GCM forced by observed SST. **Journal of Climate**, v. 3, p. 509-522. 1990.

Latif, M.; Sperber, K.; and couthors. ENSIP: **The El Niño simulation intercomparison**. CLIVAR Report. 1999.

Lau, N. C. Modeling the seasonal dependence of the atmosphere response to observed El Niños in 1962-76. **Monthly Weather Review**, v.113, p. 1970-1996. 1985.

Lau, K. M, Sud, Y.; Kim, J.; Intercomparison of hydrologic processes in AMIP GCMs. **Bulletin American Meteorological Society**, v. 77, p. 2209-2227. 1996.

Legates, D. L.; Wilmott, C. J. Mean seasonal and spatial variability in gauge corrected, global precipitation. **International Journal Climatology**, v.10, p. 111-127. 1990.

Lenters, J. D.; Cook, K. H. Simulation and diagnosis of the regional summertime precipitation climatology of South America. **Journal of Climate**, v. 8, p. 2988-3005. 1995.

Lenters, J. D.; Cook, K. H. On the origin of the Bolivian high and related circulation features of the South American climate. **Journal Atmospheric Sciences**, v. 54, p. 656-677. 1997.

Lenters, J. D.; Cook, K. H. Summertime precipitation variability over South America: role of the large-scale circulation. **Monthly Weather Review**, v. 127, p. 409-431. 1999.

Li, Z. Ensemble atmospheric GCM simulation of climate interannual variability from 1979 to 1994. **Journal of Climate**, v. 12, p. 986-1001. 1999.

Magaña, V., Webster, P., **Towards the prediction of monsoon variability**. In: CLIVAR-Conference, Paris, Dec 1-3. p.32. 1998.

Marengo, J. A. Interannual variability of surface climate in the Amazon basin. **International Journal of Climatology**, v. 12, p. 853-863. 1992.

Marengo, J. A.; Druyan, L.; Hastenrath, S. Observational and modelling studies of Amazonia interannual climate variability. **Climatic Change,** v. 23, p. 267-286. 1993.

Marengo, J. A.; Druyan, L. Validation of model improvements for the GISS GCM. **Climate Dynamics**, v. 10, p. 163-179, 1994.

Marengo, J. A.; Miller, J. R.; Russell, G. L.; Rosenzweig, C. E.; Abramopoulos, F. Calculations of river-runoff in the GISS GCM: impacts of a new-land surface

parameterization and runoff routing model on the hydrology of the Amazon basin. **Climate Dynamics,** v. 10, p. 349-361. 1994.

Mason, S.; Goddard, L.; Graham, N.; Yuleva, E.; Sun, L.; Arkin, P. The IRI Seasonal climate prediction system and the 1997/98 El Niño event. **Bulletin American Meteorological Society**, v. 80, p.1853-1874. 1999.

Matsuyama, H.; Masuda, K. Seasonal/interannual variations of soil moisture in the former USSR and its relationship to Indian Summer Monsoon rainfall. **Journal of Climate**, v. 11, p. 652-658. 1998.

McFarlane, N.; Boer, G.J.; Blanchet, J.P.; Lazare, M. The Canadian Climate Centre second generation general circulation model and its equilibrium climate. **Journal of Climate**, v.5, 1013-1044. 1992.

Neelin, D.; Battisti, D.; Hirst, A.; Wakata, Y.; Yamagata, T.; Zebiak, S. E. ENSO theory. **Journal Geophysical Research,** v. 103; p. 14261-14290. 1998.

Nepstad, D. C.; Moreira, A. G.; Alencar, A. A. **A floresta em chamas: Origens, Impactos e Prevenção de Fogo na Amazônia**. Programa Piloto para a Proteção das Florestas Tropicais do Brasil. Brasilia, Ministério do Meio Ambiente, Secretaria parea a Coordenação da Amazônia. 1999. 202 p.

Nobre, P.; Shukla, J. Variations of sea surface temperature, wind stress and rainfall over the tropical Atlantic and South America. **Journal of Climate,** v. 9, p. 2464-2479 1996.

Nobre, P.; Cavalcanti, I. F. A. Previsão Climatica Sazonal no CPTEC-A estacao chuvosa de 1995 e 1996 no Nordeste do Brasil. In: Congresso de Meteorologia Argentino N° 7. **Anais**, Buenos Aires, 2-6 set. 1996, p.351-352. 1996.

Pezzi, L.; Cavalcanti, I. F. A. Testes de sensibilidade com o modelo CPTEC/COLA usando-se dois esquemas diferentes de conveção. Congresso Brasilieiro de Meteorologia N° 11. **Anais**, Rio de Janeiro, 16-20 out. 2000, p. 3524-3529. 2000

Pandolfo, L. Observational aspects of the low-frequency intraseasonal variability of the atmosphere in middle latitudes. **Advances in Geophysics**, v. 34, p. 93-174. 1993.

Panofsky, H. A.; Brier, G. **Some applications of statistics to meteorology.** College Park, PE, USA. The Pennsylvania State University, 1968. 224 p.

Rassmusson, E. M.; Carpenter, T. H. Variations in tropical sea surface temperature and surface winds associated with the Southern Oscillation/El Niño. **Monthly Weather Review,** v. 110, p. 354-384. 1982.

Ropeleswski, C. F.; Halpert, M. S. Global and regional scale precipitation patterns associated with the El Niño/Southern Oscillation. **Monthly Weather Review,** v.115, p. 1606-1626. 1987.

Ropeleswski, C. F.; Halpert, M. S. Precipitation patterns associated with the high index phase of the Southern Oscillation. **Journal of Climate**, v.2, p. 268-284. 1989.

Rowell, D. P. Assessing potential predictability with an ensemble of multidecadal GCM simulations. **Journal of Climate**, v. 11, p.109-120, 1998.

Rowell, D.P.; Folland, C. K.; Maskell, K.; Ward, M. N. Variability of summer rainfall over tropical North Africa (1906-92): Observations and modeling. **Quarterly Journal Royal Meteorological Society**, v.121, p. 669-704. 1995.

Satyamurty, P.; Pires Bittencourt, D. Performance evaluation statistics applied to derived fileds of NWP model forecasts. **Weather and Forecasting,** v. 14, p. 726-740. 1999.

Semazzi, F.H.M.; Bums, B.; Lin, N.H; Schemm, J. K. A GCM study of the teleconnections between the continental climate in Africa and global sea surface temperature anomalies. **Journal of Climate,** v. 9, p. 2480-2497. 1996.

Shukla, J.; Paolino, D.A.; Straus, D.M.; De Witt, D.; Fennessy, M.; Kinter III, J. L.; Marx, L.; Mo, R. Dynamical seasonal prediction with the COLA atmospheric model. **Quarterly Journal Royal Meteorological Society**, v.126, p. 2265-2291. 2000a

Shukla, J.; Anderson, J.; Baumhefner, D.; Brankovic, C.; Chang, Y.; Kalnay, E.; Marx, L.; Palmer, T. N.; Paolino, D.; Ploshay, H.; Schubert, S.; Straus, D.; Suarez, M.; Tribbia, J. Dynamical seasonal prediction. **Bulletin American Meteorological Society,** v. 81, p. 2594-2606. 2000b.

Sperber, K.R.; Palmer, T.N. Interannual tropical rainfall variability in general circulation model simulations associated with the Atmospheric Model Intercomparison Project, **Journal of Climate,** v. 9, p. 2727-2750. 1996.

Sperber, K.; and Participants AMIP Modelling Groups. Are revised models better models?. A skill assessment of regional interannual variability. **Geophysical Research Letters,** v. 26, p. 1267-1270. 1999a.

Sperber, K.; Slingo, J.; Annamalai, H. **A common mode of subseasonal and interannual variability of Indian summer monsoon.** Hamburg, Germany, CLIVAR-Exchanges. 1999b, v. 4, p. 4-7

Stern, W.; Miyakoda, K.; Feasibility of seasonal forecasts inferred from multiple GCM simulations. **Journal of Climate,** v. 8, p. 1071-1085.1995.

Storch, H.V.; Zwiers, F. W. **Statistical analysis in Climate Research**. Cambridge Univ. Press. New York, 1999. 455 p.

Trenberth, K.; Branstator, G.; Karoly, D.; Kumar, A.; Lau, N-G.; Ropelewski, C. F. Progress during TOGA in understanding and modeling global teleconnections associated with tropical sea surface temperature anomalies. **Journal Geophysical Research**, v. 103, p. 14291-14324. 1998.

Wallace, J. M.; Gutzler, D. S. Teleconnections in the geopotential height field during the Northern Hemisphere winter. **Monthly Weather Review**, v. 109, p. 784-812, 1981.

Wang, X. L., Zwiers, F. W. Interannual variability of precipitation in an ensemble of AMIP climate simulations conducted with the CCC GCM2. **Journal of Climate**, v. 2, p. 1322-1355. 1999.

Ward, M. N.; Navarra, A. Pattern analysis of SST-forced variability in ensemble GCM simulations: Examples over Europe and the Tropical Pacific. **Journal of Climate,** v. 10, p. 2210-2220. 1997.

Webster, P. J.; Magaña, V. O.; Palmer, T. N.; Shukla, J.; Tomas, R. A.; Yanai, M.; Yasunari, T. Monsoons: Processes, predictability, and the prospects for prediction. **Journal Geophysical Research**, v.103, p. 14451-14510. 1998.

Xie, P.P.; Arkin, P.A. Global precipitation: a 17-year monthly analysis based on gauge observations, satellite estimates and numerical model outputs. **Bulletin American Meteorological Society**, v. 78, p. 2539-2558. 1997.

Xie, P.P.; Arkin, P.A. Global monthly precipitation estimates from satellite-observed outgoing longwave radiation. **Journal of Climate**, v.11, p. 137-164. 1998.

Yang, B.X.A.; Anderson, J. L.; Stern, W. F. Reproducible forced modes in a AGCM ensemble integrations and potential predictability of atmospheric seasonal variations in the extratropics. **Journal of Climate**, v.11, p. 2942-2959. 1998.

Zhou, J.; Lau, K. M. Does a monsoon climate exists over South America?. **Journal of Climate,** v. 11, p. 1020-1040, 1998.

Zwiers, F. W. Interannual variability and predictability in an ensemble of AMIP climate simulations conducted with the CCC GCM2. **Climate Dynamics**, v. 12, p. 825-847. 1996.